sizes of the polyplexes were not significantly affected by the branching. In addition, ζ-potentials of pDNA polyplexes with the cationic polymers were measured to examine their electric property. The ζ-potential of the pDNA polyplexes was about +10 mV at a charge ratio more than 1/1(vector/pDNA). The difference in ζ-potential value between the polymers was little in each branching. Therefore, it can be said that there is little difference in physiochemical properties of the polyplexes produced from cationic polymers with different branching.

Cytotoxicity

Cytotoxicity of the pDNA polyplexes with the 6-branching polymer to COS-1 cells was studied by the cell survival rate using the WST-8 method. As shown in (Fig. 2) the cytotoxicity of the polyplexes was negligible up to a charge ratio of 5/1 (vector/pDNA). At charge ratios more than 5/1, the cytotoxicity was gradually reduced, and it was about 60% at a charge ratio of 20/1 (vector/pDNA).

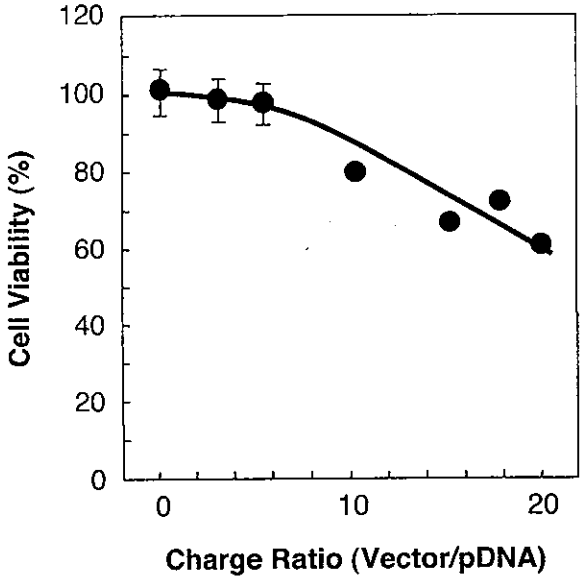

Fig. (2). Cytotoxicity of the polyplexes obtained immediately after mixing of DNA (pGL3-control) and 6-branching star polymer under the changing of a charge ratio (vector/pDNA), which was determined by cell viability assay of COS-1 cells using a WST-8 method. The data are presented as means±S.D. (n=5).

Gene Expression and Cell Viability

Gene transfer activity of the cationic polymers with same molecular weight of about 18,000 was examined and compared with that of ExGen 500 [35,36], which was one of major commercially available typical cationic polymeric vectors as a positive control. Figure 3 shows gene transfer activity of the cationic polymers at the charge ratio of 5/1 (vector/pDNA) in COS-1 cells. When pDNA alone was transfected, little luciferase activity was observed (data not shown). On the other hand, the luciferase was produced in all pDNA polyplexes. The enhancement of gene transfer activity in the use of the polyplexes may be due to acceleration of cellular uptake of pDNA polyplexes by

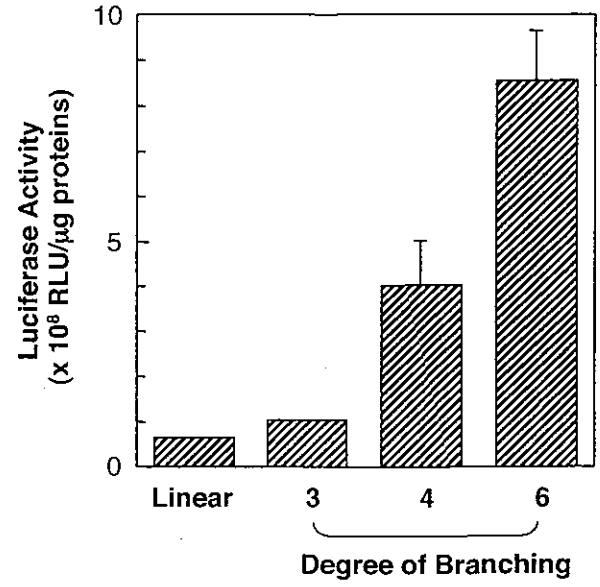

Fig. (3). Effect of branching of the star polymers on the level of luciferase gene transfer activity in COS-1 cells. COS-1 cells were treated with the polyplexes prepared by mixing of the star polymers and DNA (pGL3-control) under a charge ratio of 5/1 (vector/pDNA) 12 h after those preparation. The expression level was increased with increases in the degree of branching. The data are presented as means±S.D. (n=5).

endocytosis and endosomal release of the polyplexes by the proton sponge effect [37,38] in endosomes, similar to the other cationic polymers. The gene transfer activity of the pDNA polyplexes with the non-branched, linear cationic polymer was lowest, which was comparable with that of ExGen 500. However, the activity was increased by stage, corresponding to the degree of branching. The relative transfer activity to the linear polymer was about 2, 5 and 10 times in 3-, 4- and 6-branched polymers, respectively. As an increase in the degree of branching the transfer activity was almost exponentially increased. It can be said that the highly branched polymer called star vectors is useful for a gene delivery vector.

Cationic polymer-mediated transfection should overcome three major barriers for transfection, which includes binding of pDNA polyplexes to cell surface, endosormal release, and entry of pDNA into the nucleus. These barriers are strongly depended on the physicochemical properties of polyplexes such as net charge and particle size. Therefore, such properties markedly determine transfection efficiency. However, in the present study, transfection efficiency was strongly affected with the branching degree regardless of almost same physcochemical properties in pDNA polyplexes formed from the all branched polymers. The branching degree-dependent transfer activity changing may be estimated below. As an increase in the degree of branching the density of cationic charges in the branched polymers is increased. Higher charge density may affect the formation of higher compaction of pDNA polyplexes. The condensed pDNA polyplexes thus obtained may be stable in endosomes and also in aqueous media, which may prevent degradation

and aggregation of the polyplexes, respectively. Therefore, higher branching resulted in higher gene transfer activity.

The other star polymers as a gene delivery vector are easily designed by iniferter-based photo-living-radical polymerization. The composition of polymer chains can be determined by the kind of monomers, and the molecular weight by the irradiation time. Therefore, in addition to allowing design of the basic skeletal structure, the composition and length of polymer chains can be optimized as schematically shown in (Fig. 4). Changing the kind of monomers can control the composition of the polymer chains continuously or stepwise. To further increase the degree of branching, we will design the core molecules from benzene ring to naphthalene ring or combinations of benzene rings as multi-iniferters. Furthermore, formation of hyper branching structure by diverging of branching chains will be possible [34]. In the near future, the correlation between the three-dimensional structure in a star vector and the efficiency of gene expression will be clarified in detail.

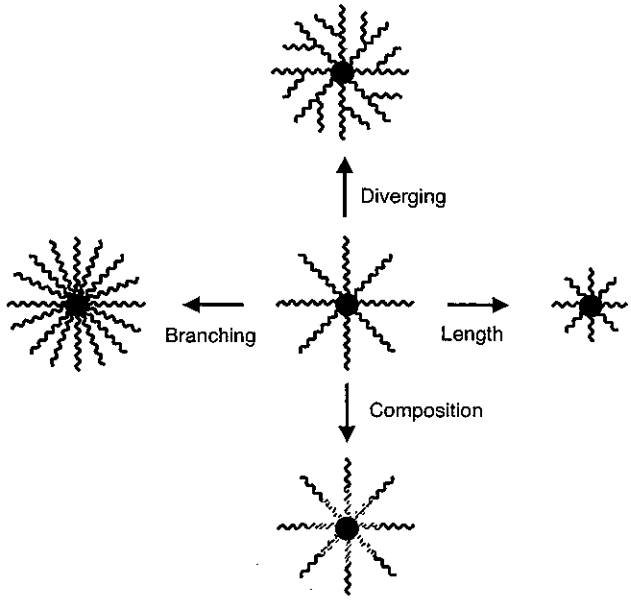

Fig. (4). Possibility in molecular design of various star polymers having different branching, diverging, chain length, or composition, which are based on iniferter-induced living radical polymerization.

ACKNOWLEDGEMENTS

This study was supported by "Research Grants for Advanced Medical Technology", "Human Genome, Tissue Engineering and Food Biotechnology", and "Aging and Health" from the Ministry of Health, Labor and Welfare of Japan, and by Grant-in-Aid for Scientific Research (B1-16390423) from the Ministry of Education, Science, Sports and Culture of Japan.

REFERENCES

[1] Felgner, P.; Barenholz, Y.; Behr, J.P.; Cheng, S.H.; Cullis, P.; Huang, L.; Jessee, F.J.; Seymour, L.; Szoka, F.; Thierry, A.R.; Wagner, E.; Wu, G. *Hum. Gene Ther.*, **1997**, *8*(5), 511-2.

[2] Niidome, T.; Huang, L. *Gene. Ther.*, **2002**, *9*(24), 1647-52.

[3] Thomas, M.; Klibanov, A.M. *Appl. Microbiol. Biotechnol.*, **2003**, *62*(1), 27-34.

[4] Gebhart, C.L.; Kabanov, A.K. *J. Control Release*, **2001**, *73*(2-3), 401-16.

[5] Nishikawa, M.; Huang, L. *Hum. Gene Ther.*, **2001**, *12*(8), 861-70.

[6] Kichise, T.; Taguchi, S.; Doi, Y. *Appl. Environ. Microbiol.*, **2002**, *68*(5), 2411-9.

[7] Zanta, M.A.; Boussif, O.; Adib, A.; Behr, J.P. *Bioconjug. Chem.*, **1997**, *8*(6), 839-944.

[8] Diebold, S.S.; Kursa, M.; Wagner, E.; Cotton, M.; Zenke, M. *J. Biol. Chem.*, **1999**, *274*(27), 19087-94.

[9] Kircheis, R.; Kichler, A.; Wallner, G.; Kursa, M.; Ogris, M.; Felzmann, T.; Buchberger, M.; Wagner, E. *Gene Ther.*, **1997**, *4*(5), 409-18.

[10] Wojda, U.; Miller, J.L. *J. Pharm. Sci.*, **2000**, *89*(5), 674-81.

[11] Li, S.; Tan, Y.; Viroonchatapan, E.; Pitt, B.R.; Huang, L. *Am. J. Physiol.*, **2000**, *278*(3), L504-11.

[12] Kurisawa, M.; Yokoyama, M.; Okano, T. *J. Control. Release*, **2000**, *69*(1), 127-37.

[13] Nagasaki, T.; Taniguchi, A.; Tamagaki, S. *Bioconjug. Chem.*, **2003**, *14*(3), 513-6.

[14] Nakayama, Y.; Umeda, M.; Uchida, K. unpublished data.

[15] Hui, S.W.; Stoicheva, N.; Zhao, Y.L. *Biophys. J.*, **1996**, *71*(2), 1123-30.

[16] Kuo, J.H.; Jan, M.S.; Sung, K.C. *Int. J. Pharm.*, **2003**, *257*(1-2), 75-84.

[17] Petersen, H.; Kunath, K.; Martin, A.L.; Stolnik, S.; Roberts, C.J.; Davies, M.C.; Kissel. T. *Biomacromolecules*, **2002**, *3*(5), 926-36.

[18] Zelikin, A.N.; Putnam, D.; Shastri, P.; Langer. R.; Izumrudov, V.A. *Bioconjug. Chem.*, **2002**, *13*(3), *548-53.*

[19] Kunath, K.; von Harpe, A.; Fischer, D.; Petersen, H.; Bickel, U.; Voigt, K.; Kissel, T. *J. Control. Release.*, **2003**, *89*(1), 113-25.

[20] Godbey, W.T.; Wu, K.K.; Mikos, A.G. *J. Biomed. Mater. Res.*; **1999**, *45*(3), 268-75.

[21] Fischer, D.; Bieber, T.; Li, Y.; Elsasser, H.P.; Kissel, T. *Pharm. Res.*, **1999**, *16*(8), 1273-79.

[22] Wightman, L.; Kircheis, R.; Rossler, V.; Carotta, S.; Ruzicka, R.; Kursa, M.; Wagner, E. *J. Gene Med.*, **2001**, *3*(4), 362-72.

[23] Van de Wetering, P., Moret, E.E.; Schuurmans-Nieuwenbroek, N.M.E.; van Streenbergen, M.J.; Hennik, W.E. *Bioconjug. Chem.* **1999**, *10*(4), 589-97.

[24] Tang, M.X.; Szoka, F.C. *Gene Ther.*, **1997**, *4*(8), 823-32.

[25] Otsu, T.; Yoshida, M, *Makromol. Chem. Rapid Commun.*, **1982**, *3*, 127-32.

[26] Otsu, T.; Yoshida, M.; Tazaki, T. *Makromol. Chem., Rapid Commun.*, **1982**, *3*, 133-40.

[27] Otsu, T.; Matsunaga, T.; Doi, T.; Matsumoto, A.; *Eur. Polym. J.*, **1995**, *31*, 67-78.

[28] Otsu, T.; Matsumoto, *Advances in Polymer Science*, **1998**, *136*, 75-137.

[29] Matyjaszewski, K. Ed. *Controlled radical polymerization.* ACS Symposium Series 685 American Chemical Society: Washington, DC, **1998**.

[30] Sawamoto, M.; Kamigaito, M. In *Polymer Synthesis; Materials Science and Technology Series*; VCH-Wiley: Weinheim, **1998**; Chapter 1.

[31] Nakayama, Y.; Matsuda, T. *Macromolecules*, **1996**, *29*(27), 8622-30.

[32] Nakayama, Y.; Matsuda, T. *Langmuir*, **1999**, *15*(17), 5560-66.

[33] Higashi, J.; Nakayama, Y.; Marchant, R.E.; Matsuda, T. *Langmuir*, **1999**, *15*(6), 2080-8.

[34] Nakayama, Y.; Sudo, M.; Uchida, K.; Matsuda, T. *Langmuir*, **2002**, *18*(7), 2601-6.

[35] Ferrari, S.; Moro, E.; Pettenazzo, A.; Behr, J.P.; Zacchello, F.; Scarpa, M. *Gene Ther.*, **1997**, *4*(10), 1100-6.

[36] Coll, J.L.; Chollet, P.; Brambilla, E.; Desplangues, D.; Behr, J.P.; Favrot, M. *Hum. Gene Ther.*, **1999**, *10*(10), 1659-66.

[37] Boussif, O.; Zanta, M.A.; Behr, J.P. *Gene Ther.*, **1996**, *3*(12), 1074-80.

[38] Sonawane, N.D.; Szoka, F.C. Jr.; Verkman, A.S. *J. Biol. Chem.*, **2003**, *278*(45), 44826-31.

Received: July 01, 2004 Accepted: August 03, 2004

Disruption of Autosomal Recessive Hypercholesterolemia Gene Shows Different Phenotype In Vitro and In Vivo

Mariko Harada-Shiba, Atsuko Takagi, Kousuke Marutsuka, Sayaka Moriguchi, Hiroaki Yagyu, Shun Ishibashi, Yujiro Asada, Shinji Yokoyama

Abstract—We previously characterized the patients with autosomal recessive hypercholesterolemia (ARH) as having severe hypercholesterolemia and retarded plasma low-density lipoprotein (LDL) clearance despite normal LDL receptor (LDLR) function in their cultured fibroblasts, and we identified a mutation in the *ARH* locus in these patients. ARH protein is an adaptor protein of the LDL and reportedly modulates its internalization. We developed ARH knockout mice ($ARH^{-/-}$) to study the function of this protein. Plasma total cholesterol level was higher in $ARH^{-/-}$ mice than that in wild-type mice ($ARH^{+/+}$), being attributed to a 6-fold increase of LDL, whereas plasma lipoprotein was normal in the heterozygotes ($ARH^{+/-}$). Clearance of ^{125}I-LDL from plasma was retarded in $ARH^{-/-}$ mice, as much as that found in $LDLR^{-/-}$ mice. Fluorescence activity of the intravenously injected 1,1′-dioctadecyl-3,3,3′,3′-tetramethylindocarbocyanine perchlorate (DiI)-LDL was recovered in the cytosol of the hepatocytes of $ARH^{+/+}$ mice, but not in those of $ARH^{-/-}$ or $LDLR^{-/-}$ mice. Also, less radioactivity was recovered in the liver of $ARH^{-/-}$ or $LDLR^{-/-}$ mice when [^{3}H]cholesteryl oleyl ether (CE)-labeled LDL was injected. In contrast, uptakes of [^{3}H]CE-labeled LDL, ^{125}I-LDL, and DiI-LDL were all normal or slightly subnormal when the $ARH^{-/-}$ hepatocytes were cultured. We thus concluded that the function of the hepatic LDLR is impaired in the $ARH^{-/-}$ mice in vivo, despite its normal function in vitro. These findings were consistent with the observations with the ARH homozygous patients and suggested that certain cellular environmental factors modulate the requirement of ARH for the LDLR function. (***Circ Res.* 2004;95:945-952.**)

Key Words: autosomal recessive hypercholesterolemia ■ knockout mouse ■ low-density lipoprotein receptor ■ primary cultured hepatocytes ■ OmniBank

Hereditary hypercholesterolemia was first characterized by Khachadurian and Kuthman in 1973[1] as severe hypercholesterolemia with cutaneous and tendon xanthomas and premature atherosclerosis. They proposed two categories, autosomal dominant and recessive.[1] Hypercholesterolemia with autosomal dominant inheritance was termed familial hypercholesterolemia. Studies of familial hypercholesterolemia led to the discovery of low-density lipoprotein receptor (LDLR) and identification of its genetic dysfunction as the cause of this disease. The LDLR is now known to play a key role in the internalization of LDL into the cell and in the regulation of plasma LDL concentrations.[2,3] However, hypercholesterolemia with autosomal recessive inheritance had never been fully characterized until we first reported this disease.[4,5] In these articles, we described siblings with severe hypercholesterolemia, exhibiting huge xanthomas and premature atherosclerosis despite normal LDLR activity in their cultured fibroblasts.

In 2001, Garcia et al[6] mapped the *ARH* locus to chromosome 1p35 using six families of autosomal recessive hypercholesterolemia (ARH). They identified six mutations of the gene encoding a putative LDLR adaptor protein in these ARH families. We showed that an insertion mutation in the *ARH* gene of the Japanese siblings described causes an early stop codon.[7]

ARH protein has an N-terminal phosphotyrosine-binding (PTB) domain.[6] The PTB domain is found in several adaptor proteins, such as Disabled-2 and numb, and binds to an NPXY sequence in the cytoplasmic tails of cell surface receptors to modulate their internalization. Recently, the PTB domain of ARH protein was shown by the pull-down technique to bind to the FDNPVY sequence of LDLR.[8] ARH protein was also reported to interact with clathrin and is thought to function as an adaptor protein that couples LDLR to the endocytic machinery.[8]

What is unique about the patients with ARH is the apparent inconsistency of the LDLR functions between in vitro and in

Original received October 24, 2003; resubmission received June 10, 2004; revised resubmission received September 13, 2004; accepted September 24, 2004.

From the Department of Bioscience (M.H.-S.), Department of Pharmacology (A.T.), National Cardiovascular Center Research Institute, Osaka; First Department of Pathology (K.M., S.M., Y.A.), Miyazaki Medical College, Miyazaki; Division of Endocrinology and Metabolism (H.Y., S.I.), Jichi Medical School, Kawachi-gun, Tochigi; Department of Biochemistry, Cell Biology, and Metabolism (S.Y.), Nagoya City University Graduate School of Medical Sciences, Mizuho-cho, Nagoya, Aichi, Japan.

Correspondence to Mariko Harada-Shiba, Department of Bioscience, National Cardiovascular Center Research Institute, Fujishiro-dai, Suita, Osaka 565-8565, Japan. E-mail mshiba@ri.ncvc.go.jp

Circulation Research is available at http://www.circresaha.org DOI: 10.1161/01.RES.0000146946.78540.46

vivo. In ARH patients, clearance of ^{125}I-LDL from plasma is delayed to the same extent as that found among homozygous familial hypercholesterolemia, whereas LDL binding, internalization, and degradation are normal or subnormal in their cultured fibroblasts.[9–11] However, a defect in LDLR internalization was observed in Epstein-Barr virus lymphocytes from ARH patients.[12] LDLR activity in these mutant cells could be restored by retrovirus-mediated expression of normal ARH.[13] The results indicated that lymphocytes require ARH for normal functioning of the LDLR even in vitro, whereas fibroblasts express the normal LDLR functions without ARH, at least in vitro. Because ARH patients have delayed clearance of LDL, the LDLR requires ARH for its functions, at least in the liver in vivo. Jones et al[14] reported that ARH-deficient mice have delayed catabolism of LDL, higher LDL cholesterol levels, and greater immunodetectable LDLR on the sinusoidal surface of hepatocytes.

In the present study, we characterized *ARH*-deficient mice to study the functions of ARH. *ARH*$^{-/-}$ mice showed a higher level of plasma LDL cholesterol than wild-type mice, whereas *ARH*$^{+/-}$ mice did not show hypercholesterolemia, being consistent with clinical manifestation of the human ARH patients.[5,7] The clearance of ^{125}I-LDL was delayed, and hepatic uptake of 1,1′-dioctadecyl-3,3,3′,3′-tetramethylindocarbocyanine perchlorate (DiI)-LDL and of [^{3}H]cholesteryl oleyl ether-labeled LDL (^{3}H-CE-LDL) was decreased in *ARH*$^{-/-}$ mice. However, primary cultured hepatocytes of *ARH*$^{-/-}$ mice had normal functions to internalize ^{3}H-CE-LDL, ^{125}I-LDL, and DiI-LDL. Thus, the results indicate that the cellular environment modulates the regulation of LDLR function by ARH protein.

Materials and Methods

General Procedure

Plasma lipoproteins were analyzed by high-performance liquid chromatography using molecular sieve columns (Skylight Biotech, Inc).[15] Cholesterol and triglycerides were measured using enzyme assay kits (Wako, Tokyo, Japan). Na^{125}I (37 GBq/mL) and [1α,2α(*n*)-^{3}H]cholesteryl oleyl ether (^{3}H-CE) (1.63 TBq/mmol) were purchased from Amersham (Buckinghamshire, UK). LDL was isolated by sequential ultracentrifugation in a density range of 1.019<density<1.064 from pooled plasma of apolipoprotein E knockout mice (Jackson Laboratory, Bar Harbor, Me) or normal human volunteers after overnight fasting. Human lipoprotein-deficient serum (LPDS) (density>1.215 g/mL) was prepared by ultracentrifugation.

Generation of Knockout Mouse

To generate *ARH* knockout mice, mutations were created by insertional mutagenesis using the gene trap vectors developed by Lexicon Genetics Incorporated (Woodlands, Tex), based on retroviral-based gene trap technology previously reported.[16] OmniBank Sequence Tag 149604 corresponded to the insertion mutation in the third intron of *ARH* gene in mouse chromosome 4 (Figure 1A). The line was obtained from Lexicon Genetics Incorporated. All experiments were performed with the F2-generation or F3-generation descendants, which were backcrossed with the C57Bl/6. LDLR knockout mice (*LDLR*$^{-/-}$) were generated as previously described,[17] which were backcrossed to C57Bl/6 mice, and were used for the study.

Southern Blot Analysis

Southern blot analysis was performed after digestion of the DNA prepared from liver with *Apa*I. ^{32}P-labeled polymerase chain reaction products (239 bp) amplified from portions of exon 3 and intron 3 of the mouse *ARH* gene with primers 5′-ATCATCCTGACCGACAGCCT-3′ and 5′-GGCACAACATAACCGACCTA-3′ or neo gene fragment (850 bp) derived from pBS64neo (Lexicon Genetics Inc) as probes according to the standard procedure.[18]

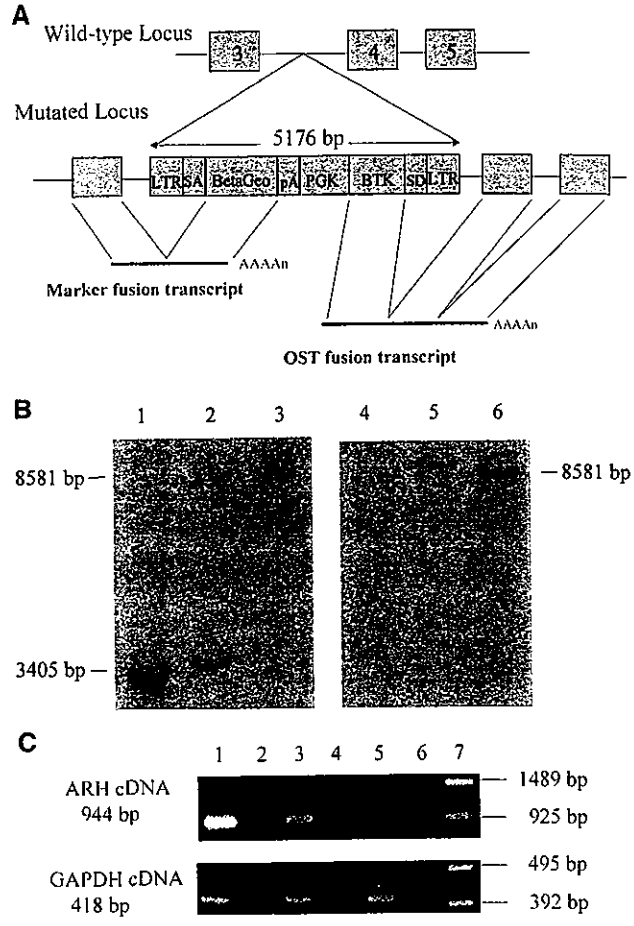

Figure 1. A, Strategy for insertional mutagenesis of the *ARH* locus in the mouse genome. The gene trap vector contains a promoterless splice acceptor sequence (SA) and BetaGeo, which create marker fusion transcripts. The vector also contains a long terminal repeat (LTR), a phosphoglycerate kinase-1 promoter (PGK), Bruton tyrosine kinase (BTK), and a splice donor sequence (SD). OmniBank Sequence Tag 149604 has an insertion of the vector in the third intron of *ARH* gene. B, Southern blot analysis of liver DNA. DNA was digested with *Apa*I and hybridized with a probe comprising portions of the mouse *ARH* gene containing exon 3 and intron 3 (lanes 1 to 3) or neo gene (lanes 4 to 6). Lanes 1 and 4, *ARH*$^{+/+}$; lanes 2 and 5, *ARH*$^{+/-}$; lanes 3 and 6, *ARH*$^{-/-}$. C, Reverse-transcription polymerase chain reaction of ARH and GAPDH mRNA. Lane 1 and 2, *ARH*$^{+/+}$; 3 and 4, *ARH*$^{+/-}$; 5 and 6, *ARH*$^{-/-}$. Lane 1, 3, and 5 are reverse-transcription plus; 2, 4, and 6 are reverse-transcription minus. Lane 7 shows size markers, lambda DNA digested with *Sty*1 for ARH, and phiX174 DNA digested with *Hin*cII for GAPDH.

Reverse-Transcription Polymerase Chain Reaction

Total RNA was isolated from the liver of wild-type, heterozygous, and homozygous mice using the acid guanidium thiocyanate-phenol-chloroform method, as described.[19]

^{125}I-LDL Turnover Study

Mouse LDL was iodinated with ^{125}I by the iodine monochloride method[20] to give a specific activity of ^{125}I-LDL >200 cpm/ng

protein. Female mice of the genotypes of wild-type ($ARH^{+/+}$), $ARH^{+/-}$, $ARH^{-/-}$, and $LDLR^{-/-}$, 12 to 15 weeks of age, were fasted for 13 hours. Three mice in each genotype received an intravenous bolus via the external jugular vein of ^{125}I-labeled mouse LDL (5 μg of protein). Blood was collected from the tail vein with heparinized Pasteur pipette at the indicated timings. The plasma ^{125}I-labeled apoB was measured by isopropanol precipitation, followed by gamma counting as previously described.[17]

In Vivo Hepatic Uptake of Intravenously Injected DiI-LDL

Twelve-week-old female mice of the genotypes of wild-type, $ARH^{-/-}$, and $LDLR^{-/-}$ were fasted for 13 hours. Each mouse received an intravenous bolus via the external jugular vein of 50 μg of human DiI-LDL (Molecular Probes Inc, Eugene, Ore). To detect nonspecific incorporation of DiI-LDL, 2.5 mg of unlabeled human LDL was injected 2 minutes before 50 μg of DiI-LDL was injected. Two minutes after DiI-LDL injection, blood was collected for determination of cholesterol and lipoproteins. After 4 hours, the right atrium was punctured, 10 mL of phosphate-buffered saline (PBS) was injected via the left ventricle, and subsequently 10 mL of PBS containing 4% paraformaldehyde. The tissues were immersed in PBS containing 4% paraformaldehyde at 4°C for 12 hours. The liver samples were frozen in liquid nitrogen and subjected to microscopic analysis. To stain Kupffer cells, BM8 (rat antibody against mouse pan-macrophage) (BMA Biomedicals AG, Augst, Switzerland) was used as a primary antibody and fluorescein isothiocyanate-conjugated rabbit anti-rat IgG (DAKO Cytomation, Glostrup, Denmark) was used as a secondary antibody. The samples were observed by confocal laser scanning microscopy (LSM5 PASCAL; Zeiss, Co, Tokyo, Japan).

Labeling of Human LDL With ^{3}H-CE

LDL was labeled with ^{3}H-CE according to the previously described method,[21] with a minor modifications.

In Vivo Hepatic Uptake of Intravenously Injected ^{3}H-CE-LDL

^{3}H-CE-LDL (0.8 μCi) was injected via the external jugular vein of wild-type ($ARH^{+/+}$), $ARH^{-/-}$, and $LDLR^{-/-}$ female mice, 12 to 15 weeks of age. Blood was collected from the tail vein with heparinized Pasteur pipette at 2 minutes and 4 hours after the injection. The blood was dispersed in chloroform/methanol, 2/1 (v/v). Immediately after the second blood collection, 2 mg of human LDL was injected via the inferior vena cava. Ten minutes later, the right atrium was punctured and 20 mL of PBS was injected via the left ventricle three times to wash the blood from the body. The liver was isolated, immersed in chloroform/methanol 2/1 (v/v), and homogenized with a polytron homogenizer. The lipid was extracted from the liver and the blood by the method of Folch.[22] Radioactivity in each sample was counted in a liquid scintillation counter using a scintillation cocktail of toluene/Triton X100 (2:1) containing PPO (0.6%) and POPOP (0.05%).

Preparation and Culture of Mouse Hepatocytes

Mice (14 to 16 weeks of age) of the indicated genotype were used for the study. The livers were perfused via the portal vein and hepatocytes were obtained by the method of Seglen.[23] After 24-hour incubation in Waymouth MB 752/1 medium containing 10% fetal calf serum in six-well plates, the cells were subjected to the study.

In Vitro Uptake of ^{3}H-CE-LDL Into Primary Cultured Hepatocytes

The cells were incubated in Waymouth MB 752/1 medium containing 10% LPDS for 48 hours, and then incubated in DMEM containing 2% bovine serum albumin (without free fatty acid) and ^{3}H-CE-LDL (5 to 100 μg/mL) for an additional 3 hours. Then, the cells were washed twice with 150 mmol/L NaCl, 50 mmol/L of Tris-HCl (pH 7.4) containing 2 mg/mL of bovine serum albumin, and once with the same buffer without bovine serum albumin. The cells were incubated with LDL-releasing buffer (50 mmol/L NaCl, 10 mmol/L Hepes (pH 7.4), containing 10 mg/mL heparin) at 4°C for 1 hour. After removal of the heparin-releasable fraction, 1 mL of hexane/isopropyl alcohol (3/2) was added to the cells to extract lipids in the cells.[24] After delipidation, the cells were dissolved in 1 N NaOH and protein concentration was measured.

^{125}I-LDL Binding, Incorporation, and Degradation Assays

Waymouth MB 752/1 medium containing 10% LPDS was added to the cells and incubated for another 24 hours. Binding, internalization, and degradation of ^{125}I-LDL were analyzed according to the method previously described.[25]

DiI-LDL Incorporation Into Primary Cultured Hepatocytes

The cells were added to Waymouth MB 752/1 medium containing 10% LPDS and incubated for 24 hours. Then, the cells were washed twice and incubated at 37°C for 3 hours with 50 μg/mL of DiI-LDL in 0.2 mL of MEM containing 10% LPDS. Nonspecific incorporation was determined by parallel incubation in the presence of 20-fold excess of LDL. The cells were washed three times with PBS containing 0.2% bovine serum albumin, followed by washing twice with PBS. The samples were observed with a laser confocal microscopy.

An expanded Materials and Methods section is available in the online data supplement at http://circres.ahajournals.org.

Results

Generation of *ARH* Knockout Mice

OmniBank Sequence Tag 149604 (Lexicon Genetics Inc) corresponded to the insertion mutation in the third intron of *ARH* gene in mouse chromosome 4 (Figure 1A). The mutated allele encodes a marker fusion transcript and OmniBank Sequence Tag fusion transcript instead of *ARH* mRNA. The offspring heterozygous animals were mated to produce $ARH^{+/+}$, $ARH^{+/-}$, and $ARH^{-/-}$ mice. Southern blot analysis was performed to genotype the mice using a probe comprising portions of mouse *ARH* gene containing both exon 3 and intron 3 (Figure 1B) after digestion of DNA with *Apa*I. *Apa*I site is not present in the insertion fragment used for development of the knockout mice. Southern blot analysis with the exon probe showed a 3405-bp band for the wild-type allele and was observed in both the wild-type and $ARH^{+/-}$ mice, whereas an 8581-bp band, the disrupted allele which was produced by the insertion of 5176-bp fragment (Figure 1A), was observed in $ARH^{+/-}$ and $ARH^{-/-}$ mice after digestion of DNA with *Apa*I. Southern blot analysis with neo gene probe demonstrated that only one position and one copy insertion event occurred in a mouse genome because $ARH^{+/-}$ and $ARH^{-/-}$ exhibited an 8581 bp.

To confirm that the mutated allele does not express the mRNA, total RNA was isolated from the livers of the animals of each genotype and analyzed by reverse-transcription polymerase chain reaction (Figure 1C). A 944-bp band, the *ARH* transcript that was expressed in wild-type and $ARH^{+/-}$ mice, was not detectable in $ARH^{-/-}$ mice. The results thus confirmed that the insertion mutation by gene trap vector disrupted the *ARH* gene expression.

TABLE 1. Lipid and Lipoprotein Profiles of ARH Knockout Mice (mean±SEM)

	Total Cholesterol, mmol/L	Triglyceride, mmol/L	HDL Cholesterol, mmol/L	LDL Cholesterol, mmol/L
Wild type				
Male (n=5)	2.68±0.14	1.04±0.26	2.49±0.12	0.17±0.05
Female (n=8)	2.57±0.22	0.78±0.07	2.20±0.19	0.30±0.04
Heterozygote				
Male (n=8)	2.92±0.14	1.00±0.13	2.78±0.11	0.13±0.03
Female (n=10)	2.82±0.19	0.76±0.06	2.40±0.14	0.35±0.08
Homozygote				
Male (n=5)	4.53±0.35†	1.20±0.10	3.10±0.52	1.01±0.21†
Female (n=8)	4.64±0.68†	1.09±0.19	2.96±0.30*	1.46±0.44*

*$P<0.05$.
†$P<0.01$ vs wild type.

Lipid and Lipoprotein Profiles of *ARH* Knockout Mice

Table 1 shows total plasma cholesterol, triglycerides, LDL cholesterol, and HDL cholesterol levels of mice from litters derived from the mating of $ARH^{+/-}$ mice fed a normal chow. Plasma total cholesterol levels were 1.8-fold higher in $ARH^{-/-}$ mice than those in $ARH^{+/+}$. The elevation of total cholesterol was attributed to the six-fold increase of LDL cholesterol. There was no significant difference in the plasma cholesterol levels between $ARH^{+/-}$ and $ARH^{+/+}$ mice. Histological analysis of the liver showed that $ARH^{-/-}$ mice at 12 weeks of age did not have fatty livers, which were observed in our ARH patients.[5]

^{125}I-LDL Turnover Study

To investigate the LDL metabolism in ARH deficiency, ^{125}I-LDL turnover study was performed in $ARH^{-/-}$, $ARH^{+/-}$, $ARH^{+/+}$ (wild-type), and $LDLR^{-/-}$ mice. The clearance of ^{125}I-LDL from circulation is demonstrated in a semilogarithmic plot in Figure 2. It was substantially retarded in $ARH^{-/-}$ and $LDLR^{-/-}$ mice compared with wild-type mice. The clearance rate of ^{125}I-LDL in $ARH^{+/-}$ mice was similar to that in wild-type mice. The half-lives of the plasma ^{125}I-LDL were 11.7 hours in $ARH^{-/-}$ and 6.0 hours in $LDLR^{-/-}$ mice, and both were longer than those in $ARH^{+/-}$ and wild-type mice (2.8 hours).

Microscopic Findings in the Liver After Injection of DiI-LDL

To study whether the delayed clearance of LDL in $ARH^{-/-}$ mice is attributable to impaired catabolism of LDL in the liver, the liver specimen was examined after injection of DiI-LDL in wild-type, $LDLR^{-/-}$, and $ARH^{-/-}$ mice (Figure 3). Kupffer cells were identified by fluorescein isothiocyanate (Figure 3B, 3D, 3F, 3H, 3J, and 3L). Fluorescence activity was detected in the cytosol of the hepatocytes and Kupffer cells in wild-type mice, indicating that both types of cells effectively take-up DiI-LDL (Figure 3A). Pre-injection of 2.5 mg LDL raised serum total cholesterol from 2.18±0.66 (mean±SD) mmol/L to 14.67±0.68 mmol/L, and LDL cholesterol from 0.21±0.07 mmol/L to 11.42±1.09 mmol/L in wild-type mice (Table 2). In this condition, the incorporation

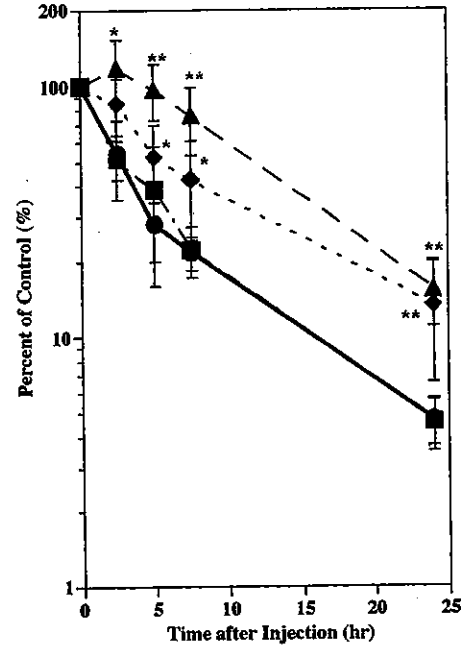

Figure 2. ^{125}I-LDL turnover study of wild-type (●), $ARH^{+/-}$ (■), $ARH^{-/-}$ (▲), and $LDLR^{-/-}$ (♦) mice. After 13 hours of fasting, wild-type, $ARH^{+/-}$, $ARH^{-/-}$, and $LDLR^{-/-}$ mice (three of each) were injected with 5 μg of ^{125}I-LDL. After the indicated time, blood was collected from the tail vein. The plasma content of ^{125}I-labeled apoB was measured by isopropanol precipitation, followed by gamma counting. The data are shown in semilogarithmic plots, and each data point represents the mean±SEM for triplicate assay. *$P<0.05$, **$P<0.01$.

of DiI-LDL into hepatocytes was decreased by the excess amount of LDL in plasma (Figure 3C), whereas its incorporation into Kupffer cells was not affected. In contrast, hepatocytes of $ARH^{-/-}$ mice were stained less extensively than those of wild-type mice by DiI-LDL fluorescence (Figure 3I), indicating that the uptake of DiI-LDL by the hepatocytes of $ARH^{-/-}$ mice was smaller than that of wild-type mice, and the presence of excess amount of LDL in plasma did not influence this result (Figure 3K). The fluorescence in the hepatocytes of $LDLR^{-/-}$ mice was also less intense than that in $ARH^{-/-}$ (Figure 3E).

In Vivo Hepatic Uptake of Intravenously Injected ^{3}H-CE-LDL

Hepatic uptake of LDL was also investigated by injecting ^{3}H-CE-LDL. Four hours after the injection, the tritium count in the blood decreased by 44% in wild-type mice, whereas it did not decrease in either $LDLR^{-/-}$ or $ARH^{-/-}$ mice (Figure 4A). The liver of wild-type mice incorporated 27.4±8.0% (mean±SD) of the injected ^{3}H-CE-LDL, whereas 9.0±1.0% was incorporated in $LDLR^{-/-}$ mice and 11.8±0.5% in $ARH^{-/-}$ mice (Figure 4B). The amount of ^{3}H-CE-LDL taken-up by the liver in $ARH^{-/-}$ was significantly smaller than that in wild-type mice but larger than that in $LDLR^{-/-}$ mice ($P<0.05$).

Incorporation of LDL in Primary Cultured Hepatocytes

In an attempt to reproduce the in vivo observations in vitro, incorporation of ^{3}H-CE-LDL was examined in primary cul-

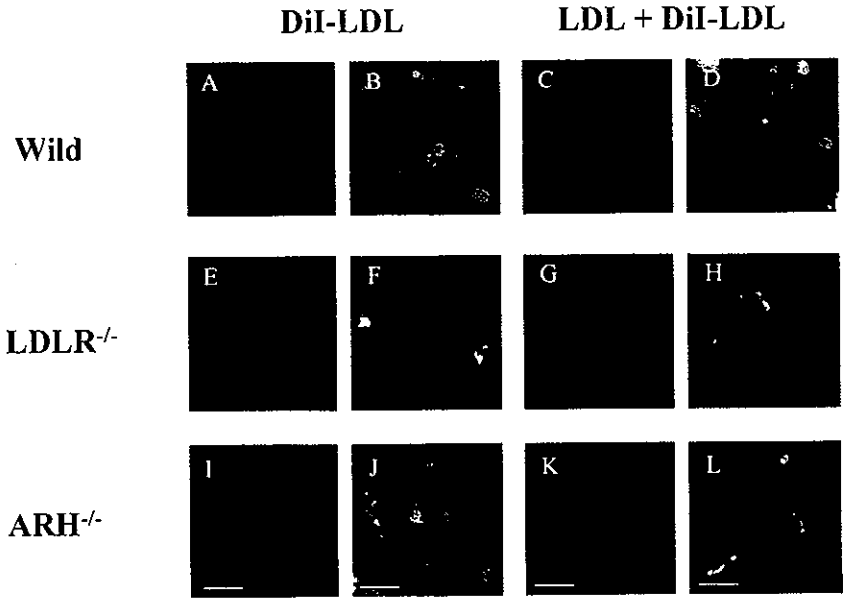

Figure 3. Microscopic findings of the liver after injection of DiI-LDL. A, E, and I, The liver from a mouse of each genotype 4 hours after the injection of 50 μg of DiI-LDL. C, G, and K, The liver from a mouse of each genotype, 4 hours after the injection of 2.5 mg of LDL, followed by 50 μg of DiI-LDL. B, F, and J, The liver from a mouse of each genotype, 4 hours after the injection of 50 μg of DiI-LDL. The specimens were stained with rat anti-mouse pan-macrophage antibody. D, H, and L, The liver from each genotype of mouse 4 hours after injection of 2.5 mg of LDL, followed by 50 μg of DiI-LDL. The specimen was stained with rat anti-mouse pan-macrophage antibody. The scale bar indicates 20 μm.

tured hepatocytes. Interestingly, the hepatocytes of $ARH^{-/-}$ mice internalized ^{3}H-CE-LDL as much as those of wild-type mice, whereas the hepatocytes of $LDLR^{-/-}$ mice took-up significantly less ^{3}H-CE-LDL (Figure 5A). The cultured hepatocytes of $ARH^{-/-}$ mice bound larger amounts of ^{125}I-LDL than those of wild-type and $LDLR^{-/-}$ mice. The hepatocytes of $ARH^{-/-}$ internalized and degraded ^{125}I-LDL as much as those of wild-type mice, which was significantly more than those of $LDLR^{-/-}$ mice (Figure 5B through 5D).

DiI-LDL Incorporation in Primary Cultured Hepatocytes

To confirm the positive incorporation of LDL by the primary cultured hepatocytes without ARH, the hepatocytes of $ARH^{-/-}$, $LDLR^{-/-}$, and wild-type mice were incubated with DiI-LDL and were observed by a laser confocal microscopy. Fluorescence-positive substances were observed in the cytosol of the hepatocytes of wild-type mice (Figure 6A), and they were suppressed in the presence of excess amounts of LDL (Figure 6B). The cultured hepatocytes of $LDLR^{-/-}$ mice showed very low fluorescence activity (Figure 6C and 6D). In contrast, the hepatocytes of $ARH^{-/-}$ mice showed fluorescence uptake of amounts similar to those observed for the wild-type (Figure 6E), and this was efficiently suppressed by excess amounts of LDL (Figure 6F).

TABLE 2. Cholesterol Levels of Total, VLDL, LDL, and HDL Fractions Before and After Administration of 2.5 mg LDL

	Total Cholesterol, mmol/L		VLDL Cholesterol, mmol/L		LDL Cholesterol, mmol/L		HDL Cholesterol, mmol/L	
	Before	After	Before	After	Before	After	Before	After
Wild-1	2.36	14.30	0.02	1.99	0.12	10.56	2.22	1.74
Wild-2	2.72	14.27	0.05	1.37	0.24	11.04	2.44	1.86
Wild-3	1.45	15.45	0.06	2.10	0.26	12.64	1.13	0.71
Mean	2.18	14.67	0.04	1.82	0.21	11.42	1.93	1.43
SD	0.66	0.68	0.02	0.39	0.07	1.09	0.70	0.63

VLDL indicates very-low-density lipoprotein.

Discussion

ARH knockout mice were developed by insertion mutation in the third intron of mouse chromosome 4. $ARH^{-/-}$ mice had a 1.8-fold higher plasma total cholesterol than wild-type litter mates fed normal chow, and this was attributed to a six-fold increase of LDL. Total cholesterol levels in $ARH^{-/-}$ mice (Table 1) were slightly lower than those reported for $LDLR^{-/-}$ mice (5.90±0.23 mmol/L in male, 6.18±0.21 mmol/L in female),[17] and cholesterol levels in $ARH^{+/-}$ mice (2.92±0.14 mmol/L in male, 2.82±0.19 mmol/L in female) were almost the same as those in $ARH^{+/+}$ mice (2.68±0.14 mmol/L in male, 2.57±0.22 mmol/L in female). The hypercholesterolemia in our $ARH^{-/-}$ mice appears to be milder than that reported by Jones et al,[14] who have recently reported that total cholesterol levels were moderately higher both in $ARH^{-/-}$ mice (7.96±1.63 mmol/L) and in $ARH^{+/-}$ mice (4.06±0.58 mmol/L) compared with that in $ARH^{+/+}$ mice (3.26±1.00 mmol/L) fed a chow containing 0.2% cholesterol. The difference in the plasma total cholesterol values between our $ARH^{-/-}$ mice and theirs may stem from different cholesterol content of the diet, because the chow we used contained 0.1% cholesterol.

The clearance of ^{125}I-LDL from the circulation was significantly delayed in $ARH^{-/-}$ mice like in $LDLR^{-/-}$ mice (Figure 2), indicating that the in vivo catabolic rate of LDL is decreased in $ARH^{-/-}$ mice. The half-life for the disappearance of ^{125}I-LDL in $ARH^{-/-}$ mice (11.7 hours) was longer than that observed in wild-type mice (2.8 hours) but not significantly different from that in $LDLR^{-/-}$ (6.0 hours). The LDL clearance in $ARH^{+/-}$ mice was same as that in the wild-type mice, suggesting that their LDL catabolism is normal. These results appear to be consistent with the findings in the ARH patients.[5]

To investigate the in vivo mechanism for the delayed catabolism of LDL directly in $ARH^{-/-}$ mice, hepatic uptake of

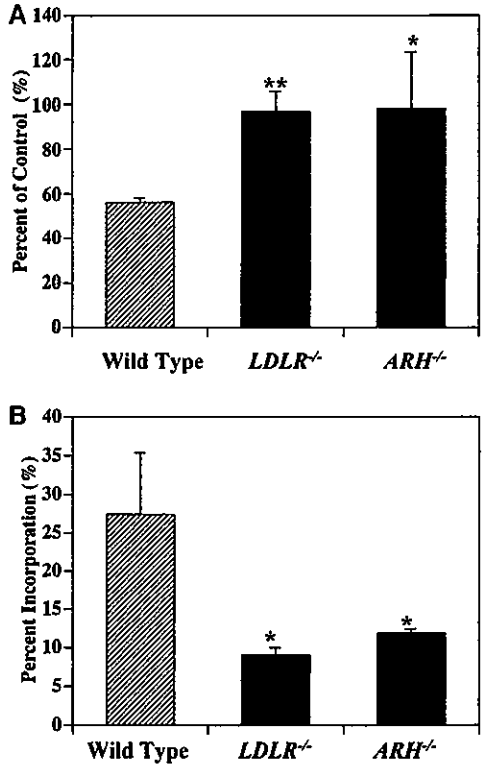

Figure 4. Hepatic uptake of intravenously injected ^{3}H-CE-LDL. ^{3}H-CE-LDL was injected into a mouse of each genotype. The blood was collected at 2 minutes and 4 hours after the injection. Immediately after the blood collection at 4 hours, 2 mg of LDL was injected and equilibrated for 10 minutes. The blood was washed from the body as described in the Methods section, and the liver was isolated. Lipid was extracted from the liver and the blood, and radioactivity was counted. Values are mean±SEM. A, Percentage of remaining tritium radioactivity in the mouse blood after 4 hours compared to that after 2 minutes. B, Hepatic uptake of tritium in the liver, 4 hours after injection, expressed as percentage of the total radioactivity injected calculated from the count in the blood at 2 minutes after the injection. *P<0.05, **P<0.01.

DiI-LDL was monitored. The fluorescence was recovered in the cytosols of both hepatocytes and Kupffer cells of wild-type mice (Figure 3A), and the fluorescence in the hepatocytes was suppressed by pretreatment with excess amounts of LDL (Figure 3C), suggesting that DiI-LDL was incorporated into the hepatocytes via the LDLR. Lower levels of DiI-LDL were found in hepatocytes of $LDLR^{-/-}$ and $ARH^{-/-}$ mice (Figure 3E, I). Because LDL cholesterol levels were higher in $ARH^{-/-}$ mice (1.01±0.21 mmol/L in male, 1.46±0.44 mmol/L in female) than that in wild-type mice (0.17±0.05 mmol/L in male, 0.30±0.04 mmol/L in female), injected DiI-LDL may become more diluted in $ARH^{-/-}$ by their own LDL. However, hepatic DiI-LDL uptake in $ARH^{-/-}$ mice was much lower than the observed uptake in wild-type mice when the excess LDL was given to raise LDL cholesterol (11.42±1.09 mmol/L). This indicates that the lower uptake of DiI-LDL in $ARH^{-/-}$ was not attributable to a dilution effect caused by their high LDL levels (Figure 3C, I).

Small numbers of cells appeared highly fluorescence-positive in the liver of mice of all the genotypes including $LDLR^{-/-}$ (Figure 3A, E, I). Their fluorescent activity was not

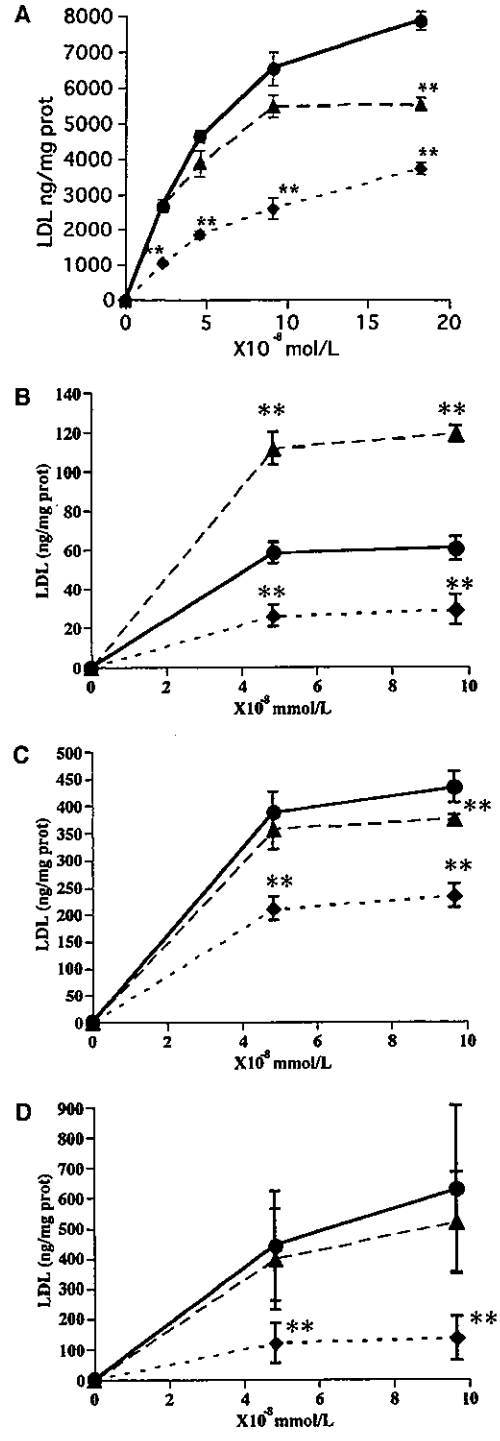

Figure 5. LDL receptor assay in primary cultured hepatocytes. Hepatocytes were obtained from the wild-type, $ARH^{-/-}$, and $LDLR^{-/-}$ mice, and cultured in Waymouth medium containing 10% fetal calf serum (day 0). On day 2, the medium was removed and the cells were washed twice. Then, the cells were cultured in Waymouth medium containing 10% LPDS. On day 3, the cells were subjected to LDL receptor assay. The data are shown as the mean±SEM of quadruplicate assays. The experiments were performed in the presence of 20-fold excess of LDL for nonspecific binding. A, ^{3}H-CE-LDL incorporation of primary cultured hepatocytes from wild-type (●), $LDLR^{-/-}$ (◆), and $ARH^{-/-}$ (▲) mice. *P<0.05, **P<0.01 vs wild-type. B, ^{125}I-LDL binding of primary cultured hepatocytes. C, ^{125}I-LDL incorporation of primary cultured hepatocytes. D, ^{125}I-LDL degradation of primary cultured hepatocytes.

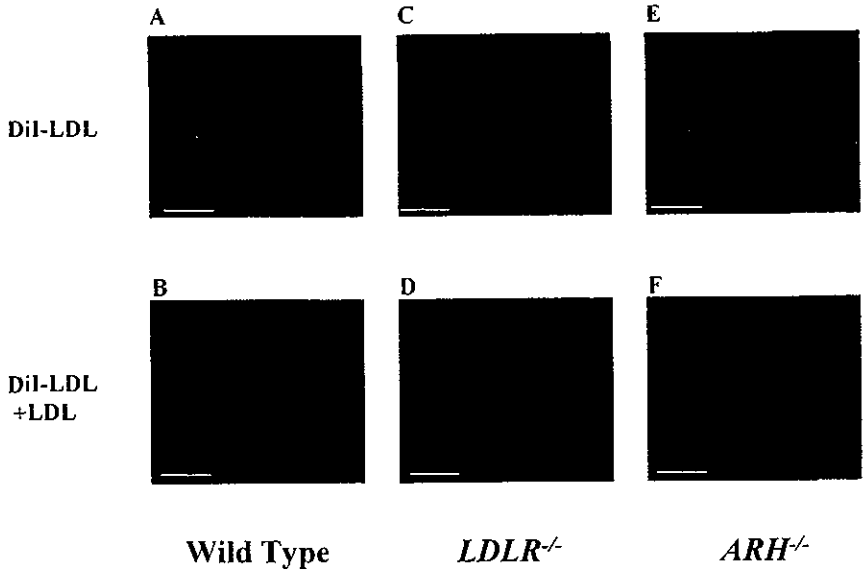

Figure 6. Dil-LDL incorporation in primary cultured hepatocytes of wild-type, $LDLR^{-/-}$, and $ARH^{-/-}$ mice. On day 0, hepatocytes were obtained from wild-type, $ARH^{-/-}$, and $LDLR^{-/-}$ mice, and cultured in Waymouth medium containing 10% fetal calf serum. After 4 hours, the cells were washed with PBS and cultured in Waymouth medium containing 10% LPDS. On day 2, the cells were incubated with Dil-LDL with or without 20 times excess of LDL for 3 hours. Then the cells were washed with PBS and mounted. A, C, and E, Hepatocytes from each genotype of mouse incubated with Dil-LDL. B, D, and F, Hepatocytes from each genotype of mouse incubated with Dil-LDL and excess of LDL. The scale bar indicates 10 μm.

decreased by the presence of excess amounts of LDL (Figure 3C, G, K) and these cells were positively identified as Kupffer cells by immunostaining with the antibody against mouse macrophages (Figure 3B, D, F, H, J, L). Thus, DiI-LDL was incorporated into Kupffer cells via an LDLR-independent pathway.

Hepatic uptake of LDL in $ARH^{-/-}$ was also examined by measuring the uptake of ^{3}H-CE-LDL by the liver. The tritium count in the blood decreased significantly in the wild-type mice, whereas it did not change in $LDLR^{-/-}$ and $ARH^{-/-}$ mice (Figure 4A). This is in agreement with the ^{125}I-LDL turnover study (Figure 2). The incorporation of ^{3}H-CE-LDL into the liver of $LDLR^{-/-}$ and $ARH^{-/-}$ mice was significantly lower than that of the wild-type mice (Figure 4B), suggesting again that the delayed turnover of LDL in $ARH^{-/-}$ mice is attributable to low LDL uptake by the liver. Interestingly, incorporation of ^{3}H-CE-LDL into the liver of $ARH^{-/-}$ is significantly higher than that of $LDLR^{-/-}$ ($P<0.05$). This result implies that the LDLR may function to incorporate LDL in the liver to some extent in vivo even without ARH.

To examine in vitro LDLR activity in the cells of $ARH^{-/-}$ mice, the incorporation of ^{3}H-CE-LDL was measured in primary cultured hepatocytes of $ARH^{-/-}$, $LDLR^{-/-}$, and wild-type mice (Figure 5A). The cultured hepatocytes of $ARH^{-/-}$ incorporated a slightly smaller amount of ^{3}H-CE-LDL than that of the wild-type, but much larger than that of $LDLR^{-/-}$. These findings were confirmed by ^{125}I-LDL incorporation and degradation experiments (Figure 5C, D). The binding of ^{125}I-LDL to the hepatocytes of $ARH^{-/-}$ was larger than that of wild-type (Figure 5B). Recently, Michaely et al[26] reported that the number of LDLRs on the cell surface of the lymphocytes in ARH subject was increased 20-fold, and that LDL binding activity was increased two-fold. The hepatocytes of $ARH^{-/-}$ seemed to remain the characteristics of in vivo status to some extent. To see whether LDL is incorporated into the cell or whether it remains on the cell surface, the cells were incubated with DiI-LDL and observed by using a laser confocal microscopy. The cytosol of the hepatocytes of $ARH^{-/-}$ mice was fluorescently stained, suggesting that DiI-LDL was internalized, like that of wild-type mice (Figure 6A, E). The results were highly consistent with the findings that the LDLR in the cultured fibroblasts from the homozygous ARH patients normally functioned, despite the fact that LDL clearance in their blood was severely impaired.[5] This suggests that the LDLR functions normally in vitro without ARH protein.

The PTB domain of ARH protein has been shown, by pull-down technique, to bind to the FDNPVY sequence of the LDLR protein.[8] ARH protein was also reported to interact with clathrin and AP-2, and it is suggested to function as an adaptor protein that couples LDLR to the endocytic machinery. ARH patients have severe hypercholesterolemia caused by delayed LDL clearance in vivo, although they have normal or subnormal levels of LDLR activity in their fibroblasts when measured in vitro.[5] However, transformed lymphocytes and monocyte-derived macrophages were unable to internalize LDL in ARH patients.[12] Thus, the dependency of LDLR function on ARH protein can be cell-specific. However, we have demonstrated here that hepatocytes do not take-up LDL in vivo without ARH protein, but they normally catabolize LDL in vitro. Thus, the requirement of ARH protein for proper functioning of the LDLR is not cell-specific, but rather may depend on the cellular environment.

Hepatic uptake of ^{3}H-CE from LDL was shown to be significantly higher in $ARH^{-/-}$ mice than $LDLR^{-/-}$ mice. This may indicate that LDLR functions to some extent without ARH, even in vivo. Some other adaptor proteins may compensate for ARH by forming an LDLR–clathrin complex, or the condition can be induced so LDLRs can be internalized without forming a clathrin complex. Our in vitro results strongly indicate that these possibilities may be enabled in a certain cellular environments.

Acknowledgments

This work was supported in part by the Promotion of Fundamental Studies in Health Science of the Organization for Pharmaceutical Safety and Research (OPSR); Research on Advanced Medical Technology from the Ministry of Health, Labour, and Welfare; Ono Medical Research Foundation; Takeda Medical Research Founda-

tion; and grant-in-aid for Scientific Research (C) (No. 15590964) from the Ministry of Education, Science, Sports, and Culture, Japan. We thank Drs Kenji Kangawa, Hisayuki Matsuo, and Hitonobu Tomoike for their helpful discussion and advice, Dr Michitaka Masuda for taking the photograph, and Dr Patrick Leahy for proofreading this manuscript. We also thank Moto Ohira, Eri Abe, Ritsuko Maeda, and Keiko Jinno for their excellent technical assistance.

References

1. Khachadurian AK, Uthman SM. Experiences with the homozygous cases of familial hypercholesterolemia. A report of 52 patients. *Nutr Metab.* 1973;15:132–140.
2. Brown MS, Anderson RG, Basu SK, Goldstein JL. Recycling of cell-surface receptors: observations from the LDL receptor system. *Cold Spring Harb Symp Quant Biol.* 1982;46(Pt 2):713–721.
3. Goldstein JL, Hobbs HH, Brown MS. Familial hypercholesterolemia. In: Scriver CR, Beaudet AL, Sly WS, Valle D, eds. *The Metabolic and Molecular Bases of Inherited Disease.* 8th ed., Vol II. New York: McGraw-Hill; 2001;2863–2913.
4. Harada-Shiba M, Tajima S, Miyake Y, Kojima S, Tsushima M, Yamamoto A. Severe hypercholesterolemia patients with normal LDL receptor. *J Jpn Atheroscler Soc.* 1991;19:227–242.
5. Harada-Shiba M, Tajima S, Yokoyama S, Miyake Y, Kojima S, Tsushima M, Kawakami M, Yamamoto A. Siblings with normal LDL receptor activity and severe hypercholesterolemia. *Arterioscler Thromb.* 1992;12:1071–1078.
6. Garcia CK, Wilund K, Arca M, Zuliani G, Fellin R, Maioli M, Calandra S, Bertolini S, Cossu F, Grishin N, Barnes R, Cohen JC, Hobbs HH. Autosomal recessive hypercholesterolemia caused by mutations in a putative LDLR adaptor protein. *Science.* 2001;292:1394–1398.
7. Harada-Shiba M, Takagi A, Miyamoto Y, Tsushima M, Ikeda Y, Yokoyama S, Yamamoto A. Clinical features and genetic analysis of autosomal recessive hypercholesterolemia. *J Clin Endocrinol Metab.* 2003;88:2541–2547.
8. He G, Gupta S, Yi M, Michaely P, Hobbs HH, Cohen JC. ARH is a modular adaptor protein that interacts with the LDL receptor, clathrin, and AP-2. *J Biol Chem.* 2002;277:44044–44049.
9. Schmidt HH, Stuhrmann M, Shamburek R, Schewe CK, Ebhardt M, Zech LA, Buttner C, Wendt M, Beisiegel U, Brewer HB, Jr, Manns MP. Delayed low density lipoprotein (LDL) catabolism despite a functional intact LDL-apolipoprotein B particle and LDL-receptor in a subject with clinical homozygous familial hypercholesterolemia. *J Clin Endocrinol Metab.* 1998;83:2167–2174.
10. Zuliani G, Arca M, Signore A, Bader G, Fazio S, Chianelli M, Bellosta S, Campagna F, Montali A, Maioli M, Pacifico A, Ricci G, Fellin R. Characterization of a new form of inherited hypercholesterolemia: familial recessive hypercholesterolemia. *Arterioscler Thromb Vasc Biol.* 1999;19:802–809.
11. Zuliani G, Vigna GB, Corsini A, Maioli M, Romagnoni F, Fellin R. Severe hypercholesterolaemia: unusual inheritance in an Italian pedigree. *Eur J Clin Invest.* 1995;25:322–331.
12. Norman D, Sun XM, Bourbon M, Knight BL, Naoumova RP, Soutar AK. Characterization of a novel cellular defect in patients with phenotypic homozygous familial hypercholesterolemia. *J Clin Invest.* 1999;104:619–628.
13. Eden ER, Patel DD, Sun XM, Burden JJ, Themis M, Edwards M, Lee P, Neuwirth C, Naoumova RP, Soutar AK. Restoration of LDL receptor function in cells from patients with autosomal recessive hypercholesterolemia by retroviral expression of ARH1. *J Clin Invest.* 2002;110:1695–1702.
14. Jones C, Hammer RE, Li WP, Cohen JC, Hobbs HH, Herz J. Normal sorting but defective endocytosis of the low density lipoprotein receptor in mice with autosomal recessive hypercholesterolemia. *J Biol Chem.* 2003;278:29024–29030.
15. Usui S, Hara Y, Hosaki S, Okazaki M. A new on-line dual enzymatic method for simultaneous quantification of cholesterol and triglycerides in lipoproteins by HPLC. *J Lipid Res.* 2002;43:805–814.
16. Zambrowicz BP, Friedrich GA, Buxton EC, Lilleberg SL, Person C, Sands AT. Disruption and sequence identification of 2,000 genes in mouse embryonic stem cells. *Nature.* 1998;392:608–611.
17. Ishibashi S, Brown MS, Goldstein JL, Gerard RD, Hammer RE, Herz J. Hypercholesterolemia in low density lipoprotein receptor knockout mice and its reversal by adenovirus-mediated gene delivery. *J Clin Invest.* 1993;92:883–893.
18. Sambrook J, Russell DW. *Molecular Cloning: A Laboratory Manual.* Cold Spring Harbor: Cold Spring Harbor Laboratory Press; 2001.
19. Nishimura N, Harada-Shiba M, Tajima S, Sugano R, Yamamura T, Qiang QZ, Yamamoto A. Acquisition of secretion of transforming growth factor-beta 1 leads to autonomous suppression of scavenger receptor activity in a monocyte-macrophage cell line, THP-1. *J Biol Chem.* 1998;273:1562–1567.
20. Bilheimer DW, Eisenberg S, Levy RI. The metabolism of very low density lipoprotein proteins. I. Preliminary in vitro and in vivo observations. *Biochim Biophys Acta.* 1972;260:212–221.
21. Nishikawa O, Yokoyama S, Okabe H, Yamamoto A. Enhancement of non-polar lipid transfer reaction through stabilization of substrate lipid particles with apolipoproteins. *J Biochem (Tokyo).* 1988;103:188–194.
22. Folch J, Lees M, Sloane Stanley GH. A simple method for the isolation and purification of total lipides from animal tissues. *J Biol Chem.* 1957;226:497–509.
23. Seglen PO. Control of glycogen metabolism in isolated rat liver cells by glucose, insulin and glucagon. *Acta Endocrinol Suppl (Copenh).* 1974;191:153–158.
24. Hara H, Yokoyama S. Interaction of free apolipoproteins with macrophages. Formation of high density lipoprotein-like lipoproteins and reduction of cellular cholesterol. *J Biol Chem.* 1991;266:3080–3086.
25. Goldstein JL, Basu SK, Brown MS. Receptor-mediated endocytosis of low-density lipoprotein in cultured cells. *Methods Enzymol.* 1983;98:241–260.
26. Michaely P, Li WP, Anderson RG, Cohen JC, Hobbs HH. The modular adaptor protein ARH is required for low density lipoprotein (LDL) binding and internalization but not for LDL receptor clustering in coated pits. *J Biol Chem.* 2004;279:34023–34031.

Adrenomedullin Gene Transfer Induces Therapeutic Angiogenesis in a Rabbit Model of Chronic Hind Limb Ischemia

Benefits of a Novel Nonviral Vector, Gelatin

Noriyuki Tokunaga, MD; Noritoshi Nagaya, MD; Mikiyasu Shirai, MD; Etsuro Tanaka, MD; Hatsue Ishibashi-Ueda, MD; Mariko Harada-Shiba, MD; Munetake Kanda, MD; Takefumi Ito, MD; Wataru Shimizu, MD; Yasuhiko Tabata, PhD; Masaaki Uematsu, MD; Kazuhiro Nishigami, MD; Shunji Sano, MD; Kenji Kangawa, PhD; Hidezo Mori, MD

Background—Earlier studies have shown that adrenomedullin (AM), a potent vasodilator peptide, has a variety of cardiovascular effects. However, whether AM has angiogenic potential remains unknown. This study investigated whether AM gene transfer induces therapeutic angiogenesis in chronic hind limb ischemia.

Methods and Results—Ischemia was induced in the hind limb of 21 Japanese White rabbits. Positively charged biodegradable gelatin was used to produce ionically linked DNA-gelatin complexes that could delay DNA degradation. Human AM DNA (naked AM group), AM DNA-gelatin complex (AM-gelatin group), or gelatin alone (control group) was injected into the ischemic thigh muscles. Four weeks after gene transfer, significant improvements in collateral formation and hind limb perfusion were observed in the naked AM group and AM-gelatin group compared with the control group (calf blood pressure ratio: 0.60±0.02, 0.72±0.03, 0.42±0.06, respectively). Interestingly, hind limb perfusion and capillary density of ischemic muscles were highest in the AM-gelatin group, which revealed the highest content of AM in the muscles among the three groups. As a result, necrosis of lower hind limb and thigh muscles was minimal in the AM-gelatin group.

Conclusions—AM gene transfer induced therapeutic angiogenesis in a rabbit model of chronic hind limb ischemia. Furthermore, the use of biodegradable gelatin as a nonviral vector augmented AM expression and thereby enhanced the therapeutic effects of AM gene transfer. Thus, gelatin-mediated AM gene transfer may be a new therapeutic strategy for the treatment of peripheral vascular diseases. (***Circulation.*** **2004;109:526-531.)**

Key Words: peripheral vascular disease ■ angiogenesis ■ gene therapy ■ ischemia

Adrenomedullin (AM) is a potent vasodilator peptide that was originally isolated from human pheochromocytoma.[1] AM and its receptor are expressed mainly in vascular endothelial cells and vascular smooth muscle cells.[2–4] AM not only induces vasorelaxation but also regulates growth and death of these vascular cells.[5–10] These findings suggest that AM plays an important role in maintaining vascular homeostasis in an autocrine and/or paracrine manner.

A recent study has shown that vascular abnormalities are present in homozygous AM knockout mice, suggesting that AM is indispensable for vascular morphogenesis.[11–13] More recently, AM has been shown to activate the PI3K/Akt-dependent pathway in vascular endothelial cells, which is considered to regulate multiple critical steps in angiogenesis, including endothelial cell survival, proliferation, migration, and capillary-like structure formation.[7,14] These results raise the possibility that AM plays a role in modulating vasculogenesis and angiogenesis. However, whether AM induces therapeutic angiogenesis remains unknown.

Received May 20, 2003; revision received September 25, 2003; accepted September 26, 2003.

From the Department of Cardiac Physiology, National Cardiovascular Center Research Institute, Osaka, Japan (N.T., M.S., M.K., H.M.); the Department of Cardiovascular Surgery, Okayama University Medical School, Okayama, Japan (N.T., S.S.); the Department of Regenerative Medicine and Tissue Engineering, National Cardiovascular Center Research Institute, Osaka, Japan (N.N., T.I.); the Department of Internal Medicine, National Cardiovascular Center, Osaka, Japan (N.N., W.S., K.N.); the Department of Physiology, the Research Center for Genetic Engineering and Cell Transplantation, Tokai University School of Medicine, Ischara, Japan (E.T.); the Department of Pathology, National Cardiovascular Center, Osaka, Japan (H.I.-U.); the Department of Biochemistry, National Cardiovascular Center Research Institute, Osaka, Japan (M.H.-S., K.K.); the Department of Biomaterials, Field of Tissue Engineering, Institute for Frontier Medical Sciences, Kyoto University, Kyoto, Japan (Y.T.); and the Cardiovascular Division, Kansai Rosai Hospital, Hyogo, Japan (M.U.).

Correspondence to Noritoshi Nagaya, MD, Department of Regenerative Medicine and Tissue Engineering or Hidezo Mori, MD, Department of Cardiac Physiology, National Cardiovascular Center Research Institute, 5-7-1 Fujishirodai, Suita, Osaka 565-8565, Japan. E-mail nagayann@hsp.ncvc.go.jp or hidemori@ri.ncvc.go.jp

Circulation is available at http://www.circulationaha.org

DOI: 10.1161/01.CIR.0000109700.81266.32

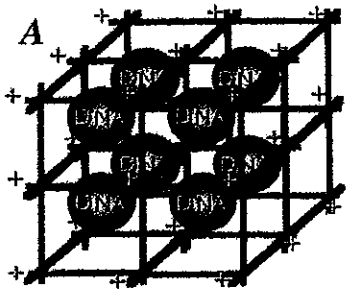

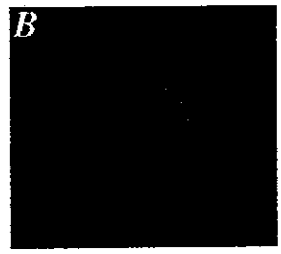

Figure 1. A, Schema of DNA-gelatin complex. Biodegradable gelatin can hold negatively charged plasmid DNA in its positively charged lattice structure. B, RITC-labeled AM DNA particles were incorporated into gelatin.

We prepared biodegradable gelatin that could hold negatively charged protein or plasmid DNA in its positively charged lattice structure.[15,16] Biodegradable gelatin has been widely used as a carrier of protein because of its capacity to delay protein degradation.[15] Similarly, ionically linked DNA-gelatin complexes can delay gene degradation.[16] These findings raise the possibility that gelatin may serve as a nonviral vector for gene therapy.

Thus, the purposes of this study were (1) to investigate whether AM gene transfer induces therapeutic angiogenesis in a rabbit model of chronic hind limb ischemia and (2) to examine whether the use of biodegradable gelatin as a vector augments AM expression and thereby enhances the therapeutic effects of AM gene transfer.

Methods

Animal Model

All protocols were performed in accordance with the guidelines of the Animal Care Ethics Committee of the National Cardiovascular Center Research Institute. Twenty-one male Japanese White rabbits (body weight, 2.9±0.1 kg; Japan Animal Co, Osaka, Japan) were used for physiological and morphological assessment. In addition, 30 rabbits were used for radioimmunoassay, immunohistochemical examination, and Western blot analysis. After anesthetization with pentobarbital sodium (30 to 35 mg/kg), a longitudinal incision was made in the left thigh, extending inferiorly from the inguinal ligament to a point just proximal to the patella. Hind limb ischemia was induced by ligation of the distal left external iliac artery and complete resection of the left femoral artery, as described previously.[17]

Construction of Plasmid DNA

To construct the expression vector for human AM, the *EcoRI/XhoI* fragment of the full-length human AM cDNA was ligated into the EcoRI/XhoI fragment of the pcDNA1.1-CMV expression plasmid (Invitrogen). To verify that the pcDNA1.1-CMV vector encoding AM cDNA produces a biologically active AM protein, the expression vector was transfected into 293 cells, and AM activity in the transfected cells was measured by high-performance liquid chromatography and radioimmunoassay. The pcDNA1.1-CMV vector encoding β-galactosidase (LacZ) cDNA was used as a control DNA.

Preparation of AM DNA-Gelatin Complex

Biodegradable gelatin was prepared from pig skin. The gelatin was characterized by a spheroid shape with a diameter of approximately 30 μm, water content of 95%, and an isoelectric point (pI) of 9 after swelling in water.[15,16] Gelatin can hold negatively charged protein or plasmid DNA in its positively charged lattice structure (Figure 1A). Dried gelatin (4 mg, pI 9) was added to human AM DNA solution (500 μg/100 μL in phosphate-buffered saline, pH 7.4). After mixture of DNA and gelatin, DNA-gelatin complexes were incubated at 37°C for 2 hours.

To visualize incorporation of DNA into gelatin, AM plasmid DNA was labeled with rhodamine B isothiocyanate (RITC), as reported previously.[16] In brief, the coupling reaction of RITC to plasmid DNA was carried out by mixing the two substances in 0.2 mol/L sodium carbonate-buffered solution (pH 9.7), followed by gel filtration with a PD 10 column (Amersham-Pharmacia). RITC-labeled AM DNA was incorporated into positively charged gelatin (Figure 1B).

Study Protocol

Ten days after the induction of hind limb ischemia (day 10), AM DNA (naked AM group, n=7), AM DNA-gelatin complex (AM-gelatin group, n=7), or gelatin alone (control group, n=7) was administered intramuscularly into 3 different sites in the ischemic adductor muscle and 2 different sites in the semimembranous muscle. In addition, Lac Z DNA-gelatin complex served as a control DNA (Lac Z-gelatin group, n=5). The amount of plasmid was 500 μg (1 mL) and that of gelatin was 4 mg. Morphological and angiographic analyses and measurements of calf blood pressure and laser Doppler flow were performed 4 weeks after gene transfer (day 38). After completion of these measurements, the adductor, semimembranous, and gastrocnemius muscles were weighed in each hind limb.[18] The muscle weight ratio was calculated for each muscle as follows: muscle weight ratio=muscle weight in ischemic hind limb/muscle weight in nonischemic hind limb. Specimens of the adductor muscle of the ischemic hind limb were obtained for histological examination.

Measurement of Calf Blood Pressure

Calf blood pressure was measured on days 10 and 38 in both hind limbs with a Doppler flowmeter (Hayashi Denki Co, Ltd) and a 25-mm-wide cuff. The pulse of the posterior tibial artery was identified with the use of a Doppler probe, and the systolic blood pressure in both hind limbs was determined by standard techniques. The calf blood pressure ratio was defined for each rabbit as the ratio of systolic pressure of the ischemic hind limb to that of the normal hind limb.[17]

Laser Doppler Blood Perfusion Analysis

Blood flow of the ischemic hind limb was measured with the use of a laser Doppler blood perfusion image system (moorLDI, Moor Instruments) on day 38.

Angiographic Analysis

Development of collateral arteries was evaluated by angiography on days 0 and 38. A 4F catheter was placed in the left internal iliac artery through the common carotid artery, and 3 mL contrast medium (Iopamiron 300, SCHERING) was injected with an automated angiography injector at a rate of 2.5 mL/s. Quantitative angiographic analysis of collateral vessel development in the ischemic hind limb was performed with the use of a 5-mm^2 grid overlay, as described previously.[17] The angiographic score was calculated for each film as the ratio of grid intersections crossed by opacified arteries divided by the total number of grid intersections in the ischemic medial thigh. The angiographic score was determined by 2 blinded observers.

Morphological and Histological Examination

The degree of lower hind limb necrosis and thigh muscle necrosis was macroscopically evaluated on graded morphological scales (grade 1 to 3) for peripheral tissue damage and muscle necrosis area of the adductor, semimembranous, and medial large muscles. Capillary density of the ischemic hind limb was evaluated by alkaline phosphatase staining, as reported previously.[17] A total of 10 different fields from three different sections were randomly selected, and the number of capillaries was counted under a ×40 objective. Capillary density was expressed as the mean number of capillaries per square millimeter. The number of myofibers in each field was also examined and the capillary/muscle fiber ratio calculated.

Radioimmunoassay for Human AM

Human AM production was examined 1, 2, and 4 weeks after gene transfer in the naked AM group, AM-gelatin group, and control group (n=5 each). The muscles were harvested for radioimmunoassay and immunohistochemical examination. Immunoreactive human AM level in rabbit muscles was determined by immunoradiometric assay with the use of a specific kit (Shionogi Co, Ltd).[19] Tissue content of vascular endothelial growth factor (VEGF) was examined by ELISA kit (R&D systems).

Immunohistochemistry for Human AM, Ki67 Antigen, and Phosphorylated Akt

Immunohistochemical studies were performed on formalin-fixed, paraffin-embedded 4-μm sections of ischemic thigh muscles 7 days after gene transfer. To elucidate AM expression after gene therapy, immunohistochemistry for human AM was performed with the use of a monoclonal antibody recognizing AM-(12–25) (1:100), as reported previously.[20] To evaluate the proliferative potential of AM, tissue sections were stained for Ki67, a marker for cell proliferation, with the use of monoclonal anti-Ki67 antibody (1:100) (DAKO). AM has recently been shown to promote proliferation of vascular endothelial cells at least in part through the PI3k/Akt pathway.[21] Thus, immunohistochemistry for phosphorylated Akt was performed with mouse monoclonal anti-phosphorylated Akt antibody (1:100) (Cell Signaling Technology).

Western Blot Analysis

To identify Akt phosphorylation in ischemic muscles after AM gene transfer, Western blotting was performed with the use of a commercially available kit (PhosphoPlus Akt [Ser473] Antibody Kit, Cell Signaling Technology). Ischemic muscles in the 3 groups were obtained 7 days after AM gene transfer. These samples were homogenized on ice in 0.1% Tween 20 homogenization buffer with a protease inhibitor (Complete, Roche). After centrifugation for 20 minutes at 4°C, the supernatant was used for Western blot analysis. The 50 μg of protein was transferred into sample buffer, loaded on 7.5% SDS-polyacrylamide gel, and blotted onto nitrocellulose membrane through the use of a wet blotting system. After blocking for 60 minutes, the membranes were incubated with primary antibodies (1:500) at 4°C overnight. The membranes were then incubated with secondary antibodies, which were conjugated with horseradish peroxidase (Cell Signaling Technology), at a final dilution of 1:2000. Signals were detected through the use of LumiGLO chemiluminescence reagents (Cell Signaling Technology).

Statistical Analysis

All results are expressed as mean±SEM. Statistical significance was evaluated by 1-way ANOVA followed by Fisher's analysis, Scheffe's F analysis, or Kruskal-Wallis test. A value of $P<0.05$ was considered statistically significant.

Results

Physiological and Morphological Assessment

Complete resection of the left femoral artery resulted in a similar decrease in calf blood pressure ratio among the 3 groups before the initiation of therapy (day 10) (Figure 2A). However, the calf blood pressure ratio on day 38 was highest in the AM-gelatin groups, followed by the naked AM group and subsequently the control group. The laser Doppler flow in hind limb was highest in the AM-gelatin group, followed by the naked AM group and the control group (Figure 2B). The calf blood pressure ratio and laser Doppler flow 4 weeks after gene transfer did not significantly differ between the control group and Lac Z-gelatin group. Lower hind limb necrosis was minimal in the AM-gelatin group, followed by the naked AM group and the control group (Figure 2C). Thigh muscle necrosis was also minimal in the AM-gelatin group. Similarly, the muscle weight ratio (ischemic/normal) on day 38 was highest in the AM-gelatin group (Table). Neither mean arterial pressure nor heart rate significantly differed among the 3 groups.

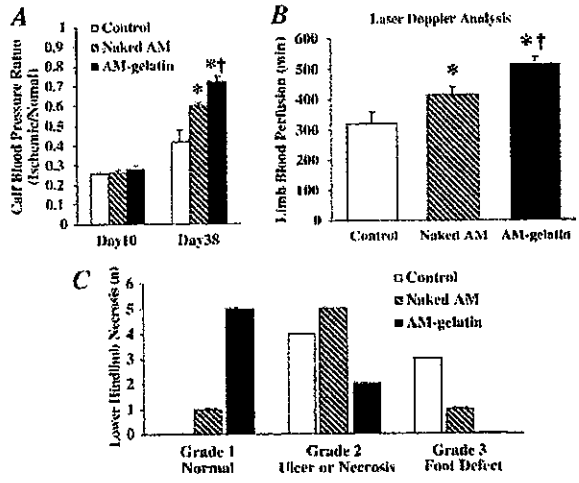

Figure 2. A, Calf blood pressure ratio (ischemic/normal hind limb) before (on day 10) and after (on day 38) gene transfer. B, Measurement of laser Doppler flow on day 38. Data are mean±SEM. *$P<0.05$ vs control group; †$P<0.05$ vs naked AM group. C, Number of cases of each grade of lower hind limb necrosis on day 38. Lower hind limb necrosis was minimal in the AM-gelatin group. Number of necrosis or foot defect is statistically significant among the 3 groups ($P<0.05$ by Kruskal-Wallis test).

Angiographic Analysis

Angiograms 4 weeks after gene transfer (day 38) showed the development of collateral arteries in the naked AM and

Physiological Characteristics

	Control	Naked AM	AM-Gelatin
No. of rabbits	7	7	7
Body weight, kg	2.46±0.06	2.65±0.10	3.16±0.09
MAP, mm Hg	112±3	114±3	116±2
HR, beats/min	269±12	253±5	262±7
Muscle weight ratio	0.71±0.03	0.84±0.02*	0.95±0.02*†

MAP indicates mean arterial pressure; HR, heart rate; and muscle weight ratio, ratio of muscle weight in ischemic hind limb to that in nonischemic hind limb. Data are mean±SEM.

*$P<0.01$ vs control group; †$P<0.05$ vs naked AM group.

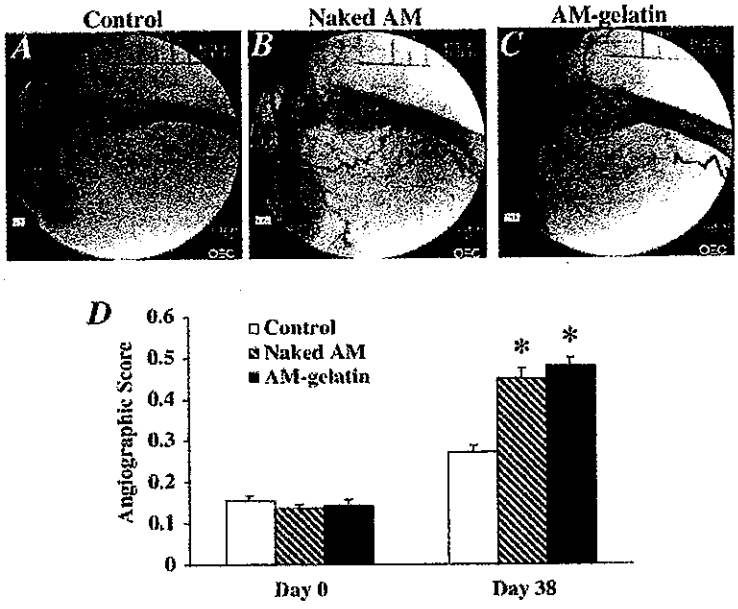

Figure 3. Representative angiograms of control group (A), naked AM group (B), and AM-gelatin group (C) on day 38. Collateral arteries were well developed in the naked AM and AM-gelatin groups. D, Angiographic score on days 0 and 38 in each group. Angiographic score on day 38 was significantly higher in the naked AM and AM-gelatin groups than in the control group. Data are mean±SEM. *$P<0.001$ versus control group.

AM-gelatin groups compared with that in the control group (Figure 3, A through C). Quantitative analysis of collateral vessels demonstrated that the angiographic score in both the naked AM and AM-gelatin groups was significantly higher than that in the control group (Figure 3D). Angiographic score did not significantly differ between the control group and Lac Z-gelatin group.

To examine the development of collateral vessels in an earlier stage, other rabbits (n=4 each) were examined 2 weeks after gene transfer (day 24). Angiograms showed significant collateral development in the naked AM and AM-gelatin groups compared with that in the control group.

Histological Examination

Alkaline phosphatase staining of ischemic hind limb muscle showed marked augmentation of neovascularization in both the naked AM and AM-gelatin groups compared with the control group (Figure 4, A through C). Quantitative analysis demonstrated that capillary density of the ischemic adductor muscle was highest in the AM-gelatin group (Figure 4D). Analysis of the capillary/muscle fiber ratio yielded similar results. Seven days after gene transfer, intense immunostaining for Ki67 was observed in vascular endothelial cells of the naked AM and the AM-gelatin groups (Figure 4, E through G).

AM Expression and Akt Phosphorylation After Gene Transfer

Seven days after gene transfer, modest immunostaining for human AM was observed in the naked AM group, whereas AM immunoreactivity was intense surrounding the gelatin in the AM-gelatin group (Figure 5, A through C). Tissue content of human AM was significantly increased both in the naked AM and the AM-gelatin groups 7 days after gene transfer (Figure 5D). The AM level in the AM-gelatin group was significantly higher that in the naked AM group. Two weeks after gene transfer, AM overexpression was observed only in the AM-gelatin group. The expression of endogenous VEGF and its receptors (Flt-1 and Flk-1) did not differ among the 3 groups (data not shown). Western blot analysis revealed that phosphorylated Akt in ischemic muscles was increased in both the naked AM and AM-gelatin groups 7 days after gene transfer (Figure 5E). Intense immunostaining for phosphory-

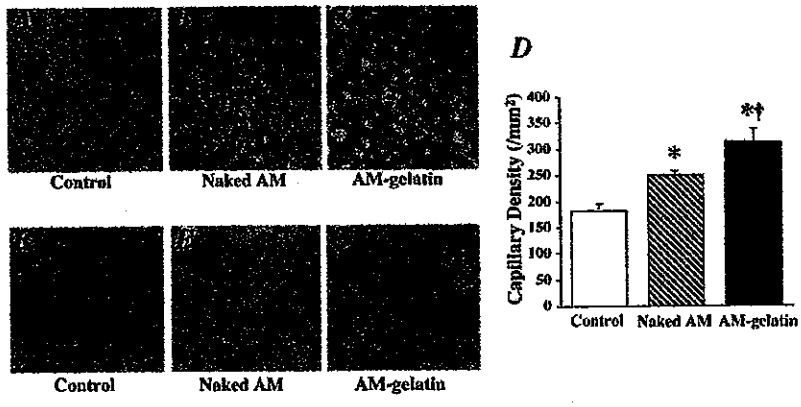

Figure 4. A through C, Representative examples of alkaline phosphatase staining in ischemic hind limb muscles. Magnification ×200. D, Quantitative analysis of capillary density in ischemic hind limb muscles. Data are mean±SEM. *$P<0.05$ vs control group; †$P<0.05$ vs naked AM group. E through G, Immunohistochemical analysis of Ki67 antigen, a marker for cell proliferation. Magnification ×400.

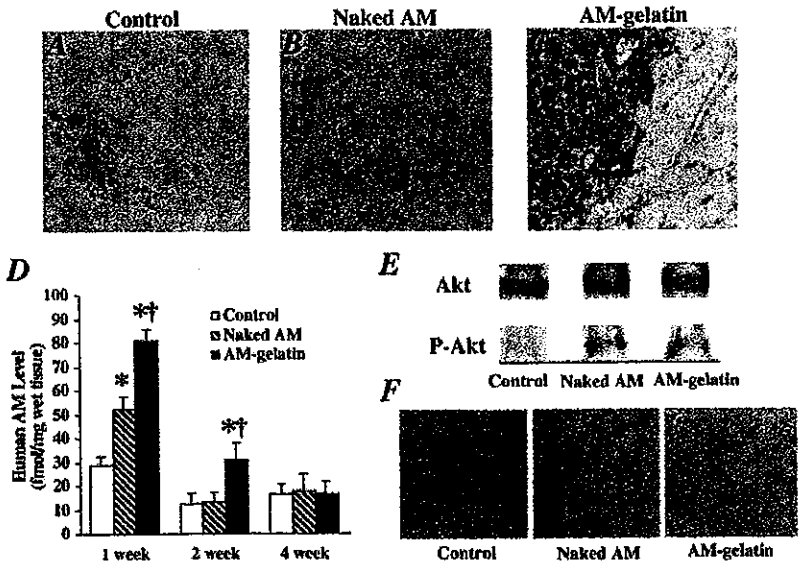

Figure 5. A through C, Immunohistochemistry for human AM 7 days after gene transfer. Intense immunostaining was observed surrounding gelatin in the AM-gelatin group. Magnification ×200. D, Time course of AM production in ischemic muscles after gene transfer. Data are mean±SEM. *$P<0.01$ vs control group; †$P<0.01$ vs naked AM group. E, Western blot analysis for Akt phosphorylation in muscles. F, Immunohistochemical staining for phosphorylated Akt 7 days after gene transfer. Phosphorylated Akt was distributed at least in endothelial cells. Magnification ×400.

lated Akt was observed at least in endothelial cells of the Naked AM and the AM-gelatin groups (Figure 5F).

Discussion

We demonstrated that (1) AM gene transfer induced hemodynamic and angiographic improvements in association with an increase in capillary density in a rabbit model of chronic hind limb ischemia. We also demonstrated that (2) administration of AM DNA-gelatin complexes markedly augmented AM expression and thereby enhanced the therapeutic effects of AM gene transfer.

AM has a variety of effects on the vasculature that include vasodilation,[1,5–7] inhibition of endothelial cell apoptosis,[8,9] and regulation of smooth muscle cell proliferation.[10] However, whether AM has angiogenic potential has remained unknown. In the present study, intramuscular administration of naked AM DNA augmented AM production in skeletal muscles, as indicated by increased tissue content and significant immunostaining of AM. As a result, AM gene transfer increased hind limb perfusion and ameliorated lower hind limb and thigh muscle necrosis in a rabbit model of hind limb ischemia. AM gene transfer may protect the ischemic hind limb partly by improving the blood flow in the ischemic hind limb because AM is originally identified as a potent vasodilating peptide.[1] Nevertheless, angiographic collateral development and high capillary density were observed in ischemic muscles after AM gene transfer. Ki67, a marker for cell proliferation, was detected in endothelial cells of microvessels after AM gene transfer. These results suggest that AM overproduction resulting from gene transfer may induce angiogenesis in a rabbit model of hind limb ischemia. Recent studies using AM gene knockout mice have shown that AM is essential for development of the vasculature during embryogenesis.[11–13] These studies support our results that AM may be an angiogenic factor. VEGF is known to induce angiogenesis and to regulate endothelial cell survival through the phosphatidylinositol 3-kinase (PI3K)/Akt pathway.[22] Thus, the PI3K/Akt pathway is considered to regulate multiple critical steps in angiogenesis, including endothelial cell survival, proliferation, migration, and capillary-like structure formation.[14] A recent study has reported that AM promotes proliferation and migration of human umbilical vein endothelial cells at least in part through the PI3K/Akt pathway.[21] The present study demonstrated that phosphorylated Akt is increased at least in endothelial cells after AM gene transfer. AM gene transfer did not influence endogenous VEGF and its receptors. Taken together, it is interesting to speculate that AM may directly induce angiogenesis through the PI3K/Akt pathway.

In the present study, we used positively charged biodegradable gelatin as a nonviral vector. We have shown that basic fibroblast growth factor (bFGF) is ionically linked with gelatin, which enhances the angiogenic effects of bFGF by delaying protein degradation.[15] Thus, biodegradable gelatin has been used as a carrier of protein. However, little information is available regarding the therapeutic potential of gelatin as a nonviral vector for gene transfer. In the present study, we demonstrated that RITC-labeled AM DNA was incorporated into positively charged gelatin. In addition, intramuscular administration of AM DNA-gelatin complexes strongly enhanced AM production compared with that of naked AM DNA. These results suggest that biodegradable gelatin may serve as a vector for gene transfer. In fact, AM DNA-gelatin complexes induced more potent angiogenic effects in a rabbit model of hind limb ischemia than naked AM DNA, as evidenced by significant increases in histological capillary density, calf blood pressure ratio, laser Doppler flow, and muscle weight ratio and a decrease in necrosis of lower hind limb and thigh muscles. These results suggest that the use of biodegradable gelatin as a nonviral vector augments AM expression and enhances AM-induced angiogenic effects. The angiogenic effects of AM-gelatin complexes were comparable to those of bFGF-gelatin complexes (data not shown). AM DNA-gelatin complexes were distributed mainly in connective tissues. We have recently demonstrated that gelatin-DNA complex is readily phagocytosed by mac-

rophages, monocytes, endothelial progenitor cells, and so on, resulting in gene expression within these phagocytes.[23,24] These findings raise the possibility that AM secreted from these cells acts on muscles in a paracrine fashion. Unlike AM production in the naked AM group, AM overexpression in the AM-gelatin group lasted for longer than 2 weeks. Thus, it is interesting to speculate that delaying gene degradation by gelatin may be responsible for the highly efficient gene transfer.

Currently, a highly efficient and safe gene delivery system is needed for gene therapy in humans. The present study demonstrated that the use of gelatin, which is considered to be less biohazardous than viral vectors, enhanced the angiogenic potential of AM DNA. Thus, gelatin-mediated AM gene transfer may be a new therapeutic strategy for the treatment of severe peripheral vascular diseases. However, the initial success of gelatin-mediated AM gene therapy reported here should be confirmed by long-term experiments, and extensive toxicity studies in animals are needed before clinical trials.

Study Limitation

First, histological capillary density, calf blood pressure ratio, and laser Doppler flow were significantly higher in the AM-gelatin group than in the naked AM group. However, the angiographic score did not significantly differ between the two. This discrepancy raises the possibility that conventional angiography may have insufficient resolution to fully visualize the angiogenic microvessels. Second, human AM level was slightly elevated in the control group. This implies that the anti-human AM antibody used in this radioimmunoassay had some cross-reactivity with endogenous rabbit AM. Nevertheless, human AM level in the muscles was highest in the AM-gelatin group within 2 weeks after gene transfer. These results suggest that AM DNA-gelatin complexes induces potent and long-lasting AM production.

Conclusions

Intramuscular administration of AM DNA induced therapeutic angiogenesis in a rabbit model of chronic hind limb ischemia. Furthermore, the use of biodegradable gelatin as a nonviral vector augmented AM expression and thereby enhanced the therapeutic effects of AM gene transfer. Thus, gelatin-mediated AM gene transfer may be a new therapeutic strategy for the treatment of peripheral vascular diseases.

Acknowledgments

This work was supported by a grant from the Japan Cardiovascular Research Foundation, HLSRG-RAMT-nano-001 and -RHGTEFB-genome-005, RGCD13C-1 from MHLW, grants from NEDO, a Grant-in-Aid for Scientific research from MECSST (13470154 and13877114), and the Promotion of Fundamental Studies in Health Science of the Organization for Pharmaceutical Safety and Research (OPSR) of Japan.

References

1. Kitamura K, Kangawa K, Kawamoto M, et al. Adrenomedullin: a novel hypotensive peptide isolated from human pheochromocytoma. *Biochem Biophys Res Commun.* 1993;192:553–560.
2. Sugo S, Minamino N, Kangawa K, et al. Endothelial cells actively synthesize and secrete adrenomedullin. *Biochem Biophys Res Commun.* 1994;201:1160–1166.
3. Sugo S, Minamino N, Shoji H, et al. Production and secretion of adrenomedullin from vascular smooth muscle cells: augmented production by tumor necrosis factor-alpha. *Biochem Biophys Res Commun.* 1994;203:719–726.
4. Kato J, Kitamura K, Kangawa K, et al. Receptors for adrenomedullin in human vascular endothelial cells. *Eur J Pharmacol.* 1995;289:383–385.
5. Shimekake Y, Nagata K, Ohta S, et al. Adrenomedullin stimulates two signal transduction pathways, cAMP accumulation and Ca^{2+} mobilization, in bovine aortic endothelial cells. *J Biol Chem.* 1995;270:4412–4417.
6. Nagaya N, Satoh T, Nishikimi T, et al. Hemodynamic, renal, and hormonal effects of adrenomedullin infusion in patients with congestive heart failure. *Circulation.* 2000;101:498–503.
7. Nishimatsu H, Suzuki E, Nagata D, et al. Adrenomedullin induces endothelium-dependent vasorelaxation via the phosphatidylinositol 3-kinase/Akt-dependent pathway in rat aorta. *Circ Res.* 2001;89:63–70.
8. Kato H, Shichiri M, Marumo F, et al. Adrenomedullin as an autocrine/paracrine apoptosis survival factor for rat endothelial cells. *Endocrinology.* 1997;138:2615–2620.
9. Sata M, Kakoki M, Nagata D, et al. Adrenomedullin and nitric oxide inhibit human endothelial cell apoptosis via a cyclic GMP-independent mechanism. *Hypertension.* 2000;36:83–88.
10. Kano H, Kohno M, Yasunari K, et al. Adrenomedullin as a novel antiproliferative factor of vascular smooth muscle cells. *J Hypertens.* 1996;14:209–213.
11. Shindo T, Kurihara Y, Nishimatsu H, et al. Vascular abnormalities and elevated blood pressure in mice lacking adrenomedullin gene. *Circulation.* 2001;104:1964–1971.
12. Caron KM, Smithies O. Extreme hydrops fetalis and cardiovascular abnormalities in mice lacking a functional adrenomedullin gene. *Proc Natl Acad Sci U S A.* 2001;98:615–619.
13. Imai Y, Shindo T, Maemura K, et al. Evidence for the physiological and pathological roles of adrenomedullin from genetic engineering in mice. *Ann N Y Acad Sci.* 2001;947:26–34.
14. Shiojima I, Walsh K. Role of Akt signaling in vascular homeostasis and angiogenesis. *Circ Res.* 2002;90:1243–1250.
15. Tabata Y, Hijikata S, Muniruzzaman M, et al. Neovascularization effect of biodegradable gelatin microspheres incorporating basic fibroblast growth factor. *J Biomater Sci Polym Ed.* 1999;10:79–94.
16. Fukunaka Y, Iwanaga K, Morimoto K, et al. Controlled release of plasmid DNA from cationized gelatin hydrogels based on hydrogel degradation. *J Control Release.* 2002;80:333–343.
17. Takeshita S, Zheng LP, Brogi E, et al. Therapeutic angiogenesis: a single intraarterial bolus of vascular endothelial growth factor augments revascularization in a rabbit ischemic hindlimb model. *J Clin Invest.* 1994;93:662–670.
18. Van Belle E, Witzenbichler B, Chen D, et al. Potentiated angiogenic effect of scatter factor/hepatocyte growth factor via induction of vascular endothelial growth factor. *Circulation.* 1998;97:381–390.
19. Ohta H, Tsuji T, Asai S, et al. A simple immunoradiometric assay for measuring the entire molecules of adrenomedullin in human plasma. *Clin Chim Acta.* 1999;287:B131–B143.
20. Nagaya N, Nishikimi T, Yoshihara F, et al. Cardiac adrenomedullin gene expression and peptide accumulation after acute myocardial infarction in rats. *Am J Physiol Regul Integr Comp Physiol.* 2000;278:R1019–R1026.
21. Miyashita K, Itoh H, Sawada N, et al. Adrenomedullin promotes proliferation and migration of cultured endothelial cells. *Hypertens Res.* 2003;26:S93–S98.
22. Jiang BH, Zheng JZ, Aoki M, et al. Phosphatidylinositol 3-kinase signaling mediates angiogenesis and expression of vascular endothelial growth factor in endothelial cells. *Proc Natl Acad Sci U S A.* 2000;97:1749–1753.
23. Tabata Y, Ikada Y. Macrophage activation through phagocytosis of muramyl dipeptide encapsulated in gelatin microspheres. *J Pharm Pharmacol.* 1987;39:698–704.
24. Nagaya N, Kangawa K, Kanda M, et al. Hybrid cell-gene therapy for pulmonary hypertension based on phagocytosing action of endothelial progenitor cells. *Circulation.* 2003;108:889–895.

Changes in Lipoprotein Profile after Selective LDL Apheresis

Key words: hypercholesterolemia, low-density lipoprotein, apheresis

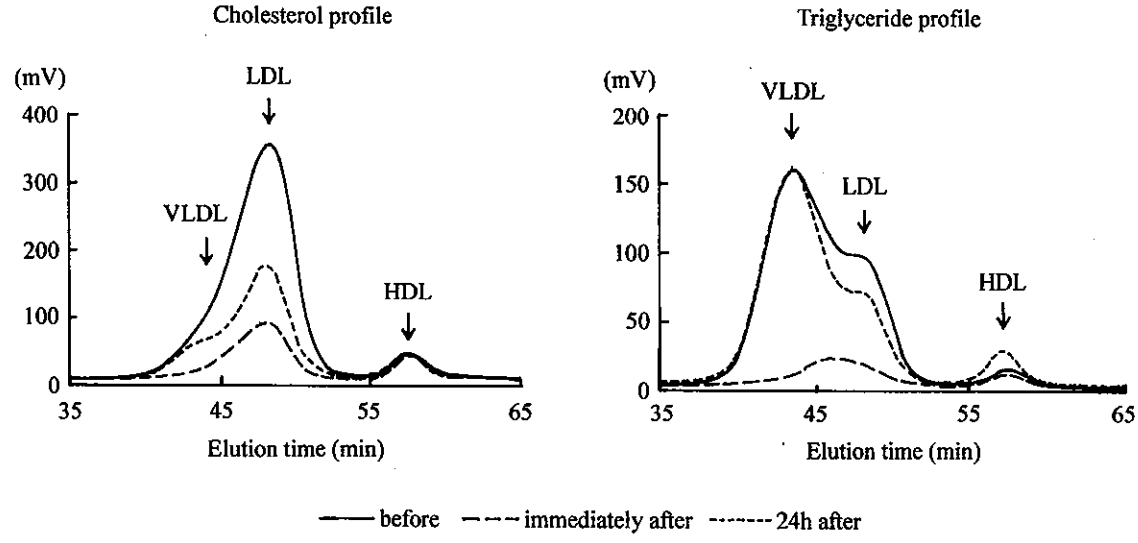

Figure 1. Left panel: Lipoprotein profile of cholesterol. Both LDL and VLDL components were prominently reduced after apheresis and half of the pre-apheresis level was noted within 24 hours, with no changes in HDL. Right panel: Lipoprotein profiles of triglyceride. Both LDL and VLDL components were prominently reduced after apheresis and the pre-apheresis level was reached within 24 hours along with doubling of the HDL component.

Low-density lipoprotein (LDL) apheresis has been used to treat patients with severe inherited forms of hypercholesterolemia. This procedure selectively removes apolipoprotein B-containing particles such as LDL, very-low density lipoprotein (VLDL), and lilpoprotein(a) [Lp(a)]. However, lipoprotein profiles of both cholesterol and triglyceride are less well understood. A 33-year-old Japanese woman with homozygous familial hypercholesterolemia was treated once a week with selective LDL filtration from the age of 28 years old. Large xanthomas occurred on the eyelid, elbow, and both sides of the knee. The plasma levels of total cholesterol, triglyceride, and Lp(a) were reduced from 390 to 121, from 322 to 27 and from 13 to 5 mg/dl immediately after apheresis (LIPOSORBER™ system) using dextran sulfate cellulose columns. HPLC analyses (CCP & 8010 series, Tosoh, Tokyo) of plasma before and after apheresis clearly showed a marked reduction of LDL and VLDL, not only of cholesterol but also triglyceride components (Fig. 1). A rebound phenomenon after 24 hours was more rapid for triglyceride than for cholesterol components.

Tomohito MATSUNAGA, Satoshi TAKASAKI, Ikuto MASAKANE, Mitsuyo OKAZAKI* and Hitonobu TOMOIKE**

Department of Cardiology, Pulmonology and Nephrology; Course of Internal Medicine and Molecular Therpeutics, Yamagata University School of Medicine, Yamagata, *Laboratory of Chemistry, College of Liberal Arts and Sciences, Tokyo Medical and Dental University, Chiba and **National Cardiovascular Center, Osaka, Japan

Received for publication March 8, 2004; Accepted for publication April 20, 2004

Reprint requests should be addressed to Dr. Hitonobu Tomoike, National Cardiovascular Center, 5-7-1 Fujishirodai, Suita, Osaka 565-8565

ELSEVIER

Atherosclerosis 173 (2004) 301–307

ATHEROSCLEROSIS

www.elsevier.com/locate/atherosclerosis

Identification of 21 single nucleotide polymorphisms in human hepatocyte growth factor gene and association with blood pressure and carotid atherosclerosis in the Japanese population

Shin Takiuchi [a,*], Toshifumi Mannami [b], Toshiyuki Miyata [c], Kei Kamide [a], Chihiro Tanaka [c], Yoshihiro Kokubo [b], Yuko Koyama [b], Nozomu Inamoto [b], Tomohiro Katsuya [e], Naoharu Iwai [c], Yuhei Kawano [a], Toshio Ogihara [e], Hitonobu Tomoike [d]

[a] *Division of Hypertension and Nephrology, Department of Medicine, National Cardiovascular Center, 5-7-1, Fujishirodai, Suita, Osaka 565-8565, Japan*

[b] *Division of Preventive Cardiology, National Cardiovascular Center, Suita, Osaka, Japan*

[c] *Research Institute, National Cardiovascular Center, Suita, Osaka, Japan*

[d] *Department of Medicine, National Cardiovascular Center, Suita, Osaka, Japan*

[e] *Department of Geriatric Medicine, Osaka University Graduate School of Medicine, Suita, Osaka, Japan*

Received 21 July 2003; accepted 15 December 2003

Abstract

It has been suggested that circulating concentrations of hepatocyte growth factor (HGF) are increased in individuals with vascular endothelial damage, such as in hypertensive patients and subjects with atherosclerosis. Because the influence of genetic variation of *HGF* has not been examined, we identified single nucleotide polymorphisms (SNPs) in the *HGF* gene, and investigated the association between these SNPs and blood pressure or carotid atherosclerosis in the Japanese general population. We identified 21 SNPs in the *HGF* gene by direct sequencing in a test population of 32 Japanese subjects. Among them, considering allele frequency and linkage disequilibrium, three SNPs, *C-1652T* in the promoter, *T43839A* in intron 8, and *T44222C* in intron 9, were genotyped in 2412 members of the Japanese general population randomly selected from the residents in Suita city. None of the three SNPs were significantly associated with blood pressure. After adjusting for age, smoking habits, consumption of alcohol, and the presence of diabetes mellitus and dyslipidemia, female subjects with the T allele of *T43839A* had more severe carotid atherosclerosis compared to individuals with the A allele. This study provides the first evidence that *HGF* may be a candidate susceptibility loci that affects the progression of atherosclerosis in Japanese subjects.

Keywords: Hepatocyte growth factor; Hypertension; Atherosclerosis; Genetics; Polymorphism

1. Introduction

Endothelial cell dysfunction has been suggested as the initiating process in the development and progression of cardiovascular disease, and it is considered to be closely related to the pathophysiology of human essential hypertension. There has been accumulating evidences that hepatocyte growth factor (HGF), mesenchyme-derived pleiotropic factor, plays an important role in endothelial cell dysfunction. Since HGF was originally identified in the plasma of rats after partial hepatectomy [1], a number of investigations have suggested that HGF is a multifunctional factor implicated in tissue regeneration and angiogenesis in not only liver but also other tissues [2,3]. A local HGF system (HGF and its receptor, c-met) is expressed in vascular cells [4], and elevated serum HGF levels have been suggested to play a cardiovascular protective role in hypertensive subjects, especially those with concomitant arteriosclerosis [5–9].

Although an association between HGF and the severity of hypertension was established, few reports have investigated the association between *HGF* gene polymorphisms and blood pressure or atherosclerosis. The *HGF* gene is composed of 18 exons encompassing 70 kb on chromosome 7q11.2-q21 [10]. In the present study, we screened for sin-

* Corresponding author. Tel.: +81-6-6833-5012; fax: +81-6-6872-7486.
E-mail address: takiuchi@hsp.ncvc.go.jp (S. Takiuchi).

0021-9150/$ – see front matter © 2004 Elsevier Ireland Ltd. All rights reserved.
doi:10.1016/j.atherosclerosis.2003.12.020

gle nucleotide polymorphisms (SNPs) in the *HGF* gene and evaluated the significance of SNPs in high blood pressure and carotid atherosclerosis determined by an ultrasonography using a large cohort, the Suita Study, which was representative of the general Japanese population.

2. Methods

2.1. Subjects

The protocol of the Suita Study, described elsewhere [11–14], was approved by the Ethics Committee of the National Cardiovascular Center. The sample consisted of 14,200 Japanese men and women ages 30–79 years stratified by gender and 10-year age groups, selected randomly from the municipal population registry. They were all invited by letter to attend regular cycles (every 2 years) of follow-up examinations. DNA from leukocytes was collected from participants who visited the Division of Preventive Medicine, National Cardiovascular Center between May 1996 and February 1998. Subjects who gave their written informed consent for genetic analyses of the genes were included in the present study. All clinical data and genotyping results were anonymous, and all data was handled in such a way that it was/will not be possible to identify an individual.

The characteristics of the subjects analyzed in the present study are summarized in Table 1. Blood pressure was measured in the subjects after at least 10 min of rest in a sitting position. Systolic blood pressure (SBP) and diastolic blood pressure (DBP) values are the mean of two physician-obtained measurements (recorded >3 min apart). Hypertension was defined as SBP ≥140 mm Hg or DBP ≥90 mm Hg or the current use of antihypertensive medications; diabetes mellitus was defined as fasting blood glucose ≥126 mg/dl, or the current use of insulin or oral anti-diabetic agents; and dyslipidemia was defined total cholesterol ≥220 mg/dl or the current use of antidyslipidemia medication at the time of the first examination.

Table 1
Clinical Features of Study Participants

Variables	Men n = 1158	Women n = 1254
Age, y	61.0 ± 12.2*	58.9 ± 11.7
Body mass index, kg/m2	23.1 ± 2.8*	22.3 ± 3.1
Systolic blood pressure (SBP), mmHg	129.2 ± 10.1	128.5 ± 21.1
Diastolic blood pressure (DBP), mmHg	81.0 ± 10.9*	78.8 ± 10.6
Total cholesterol (TC), mg/dL	204.6 ± 31.9	215.9 ± 32.9*
HDL cholesterol, mg/dL	54.1 ± 14.5	64.2 ± 15.6*
Current alcohol consumer (%)	38.0†	8.6
Current smoker (%)	71.5†	29.1
Hypertension (%)	39.6†	35.5
Diabetes mellitus (%)	9.1†	3.7
Dyslipidemia (%)	35.2	51.3†

Values are means ± SDs or percentages.
Hypertension indicates SBP ≥ 140 mmHg and/or DBP ≥90 mmHg or antihypertensive medication; Dyslipidemia, TC ≥ 220 mg/dL or antidyslipidemia medication; diabetes mellitus, fasting plasma glucose ≥ 126 mg/dL or antidiabetic medication.
* $P < 0.05$ between men and women by Student's t test.
† $P < 0.05$ between men and women by χ^2 test.

2.2. Evaluation of carotid atherosclerosis

Carotid ultrasonography was performed for the evaluation of atherosclerosis. Measurement methods were previously described [11,12]. Briefly, ultrasonography of both carotid arteries was performed with a high-resolution Duplex scanner (TOSHIBA SSA-250A; probe, SMA-736S mechanical sector scanner, Toshiba, Tokyo, Japan) for the B-scan. The subjects were examined in the supine position with their head slightly turned from the sonographer. All measurements were performed by two trained sonographers, who were unaware of the subjects' clinical data. The carotid arteries were carefully examined with regard to wall changes from different longitudinal (anterior oblique, lateral, and posterior oblique) and transverse views, and measurements of thickness were performed from transverse image. Intima-medial thickness (IMT) was measured at a point 10 mm proximal from the beginning of the dilatation of the carotid bulb, and Maximum-IMT (Max-IMT) was defined as the maximum thickness of intima-media including plaques from the region branching off from the brachiocephalic artery (right) or aorta (left) to the bifurcation of the common carotid artery. Plaque Score was calculated by summing the maximum thickness of all the plaques in the bilateral carotid artery in the scanning area [11,12].

2.3. Direct sequencing for the detection of polymorphisms in the HGF genes

We obtained peripheral blood samples from 32 Japanese volunteers for direct sequencing of the *HGF* gene after obtaining written informed consent. Genomic DNA was extracted with an NA-3000 nucleic acid isolation system (KURABO, Osaka, Japan). Methods of direct sequencing are described previously [15]. Briefly, all exons, a portion of introns and a region up-stream of exon 1, which included the promoter region of *HGF*, were amplified by polymerase chain reaction (PCR). The PCR products were then treated with shrimp alkaline phosphates and exonuclease I (PCR Product Pre-Sequencing Kit, USB Corporation, Cleveland, OH), and used as templates for direct single-pass sequencing using a BigDye Terminator v3.0 Cycle Sequencing Ready Reaction kit (Applied Biosystems, Foster City, CA). The reaction products were purified with a DyeEX 96 kit (QIAGEN) and analyzed on an ABI PRISM 3700 DNA analyzer (Applied Biosystems). The obtained sequences

Table 2
Primers and TaqMan Probes for Genotype Determination

HGF SNPs	Sequence
C(−1652)T (promoter)	
Sense	5′-GGATTAGCAATAGAAACGGGTCAT-3′
Antisense	5′-CCCTGAGGTTGTGGGATATCTAGA-3′
Probe for C(−1652)	Fam-5′-AAAATAGATCCCTCAAAAG-3′-MGB
Probe for T(−1652)	Vic-5′-AATAGATCTCTCAAAAGG-3′-MGB
A43839T (intron 8)	
Sense	5′-TTCAGTAATTTGGGCAGAGTCAGT-3′
Antisense	5′-ACGTTGGTGAAGTCAGCGCTAT-3′
Probe for A43839	Fam-5′-AGTCCAAAAAGTTAGAACT-3′-MGB
Probe for T43839	Vic-5′-AGTCCAAAATGTTAGAAC-3′-MGB
C44222T (intron 9)	
Sense	5′-GCTGGCTTGCAAACAAAATCA-3′
Antisense	5′-GGCTTAGAACTGTGGCTGTCAGT-3′
Probe for C44222	Fam-5′-TTTGAAGCTGGATTTT-3′-MGB
Probe for T44222	Vic-5′-TTGAAGTTGGATTTTT-3′-MGB

were examined for the presence of a polymorphism using Sequencher software (Gene Codes Corporation, Ann Arbor, MI), followed by visual inspection.

2.4. Genotyping of SNPs in the HGF genes

Three SNPs were genotyped using the TaqMan system [14,16]. PCR primers and probes for the TaqMan system are shown in Table 2. Fluorescence level of the reaction products was measured by use of ABI PRISM 7700 or 7900 Sequence Detection System (Applied Biosystems).

2.5. Statistical analysis

Values are expressed as the mean ± S.D. or mean ± S.E. Multiple regression and multiple logistic analyses were performed with the covariates age, body mass index, smoking, current alcohol consumption, presence of diabetes and/or dyslipidemia using the SAS version 6.0 (SAS Institute Inc., Cary, NC). Differences in frequency among the groups were tested by χ^2 analysis. Linkage disequilibrium was evaluated by obtaining r^2 values between polymorphisms using SNPAlyze ver. 2.0 (DYNACOM Co., Ltd., Shigehara, Japan).

3. Results

3.1. Detection of genetic variants in the HGF gene

We systematically searched the sequences obtained for SNPs in 32 volunteer subjects and identified 21 SNPs including 8 SNPs in the HGF promoter, 1 SNP in exon and 12 SNPs in intron regions (Table 3). Ten of these SNPs have been deposited in the public database previously, db SNPs (http://www.ncbi.nlm.nih.gov/SNP/), but 11 of the identified SNPs were novel. Thirteen SNPs had their minor allelic frequency less than 10%, therefore no further studies of these SNPs were undertaken. Six SNPs were in tight linkage disequilibrium, therefore one of them, C44222T, was selected as a representative. Thus, three SNPs, *C(-1652)T*, *A43839T* and *C44222T* were chosen for further genotyping analysis (Table 3).

Table 3
List of 21 Polymorphisms and Alele Frequency in HGF Identified in 32 Japanese Patients by Direct Sequencing

allele 1/allele 2			allele 1		allele 2		allele frequency			
SNPs	aa info.	region	homo	hetero	homo	total	allele 1	allele 2	flanking sequence	dbSNP ID
C(−2142)A		promoter	28	4	0	32	0.938	0.063	ttggaatggggt[c/a]ttatgagctacg	
G(−1965)T		promoter	31	1	0	32	0.984	0.016	atgcctcgcctt[g/t]ggggagaatgaa	
G(−1903)A		promoter	30	1	0	31	0.984	0.016	gctgattctgag[g/a]tcttcatttggg	
C(−1652)T		promoter	10	16	5	31	0.581	0.419	ataaaatagatc[c/t]ctcaaaaggaat	rs3735520
G(−1268)C		promoter	30	1	0	31	0.984	0.016	tctctgaatcaa[g/c]tgaggggtctgg	rs3735521
–(−1215)C		promoter	27	4	0	31	0.935	0.065	taggagtccccc[-/c]atgcccatacaa	
T(−955)C		promoter	31	1	0	32	0.984	0.016	ggacaatgactg[t/c]ttcttggacttt	
T(−578)C		promoter	31	1	0	32	0.984	0.016	aactagacagat[t/c]aggagctggggc	
T40171–*		intron7	0	7	25	32	0.109	0.891	taagttttttt[t/-]gttgttgttttt	rs5745686
A43839T		intron8	17	14	1	32	0.750	0.250	ctgagtccaaaa[a/t]gttagaactcta	rs2286194
C44222T*		intron9	0	7	25	32	0.109	0.891	ccaagtttgaag[c/t]tggatttttctt	rs2887069
C49065T*		intron9	0	7	25	32	0.109	0.891	acttgtaaaaaa[c/t]cttttgtttta	
T49080C*		intron9	0	7	25	32	0.109	0.891	ttttgttttatc[t/c]gccttgatattc	
A52603G*		intronl0	0	6	26	32	0.094	0.906	cctgttgtttcc[a/g]cagtcatatctt	rs1800793
G58294A		intron11	31	1	0	32	0.984	0.016	gcctgggtgaca[g/a]aatgagactctg	
T59941A		intron13	31	1	0	32	0.984	0.016	agggcacctggg[t/a]gaggcagtaaaa	rs5745739
T59984G*		intron13	26	6	0	32	0.906	0.094	tgcttgccagac[t/g]gtaagctctgga	rs2074725
G62753T		intron14	31	1	0	32	0.984	0.016	tttgctcttaag[g/t]ttataatatgta	rs5745745
G63555T	Asp543Tyr	exonl5	31	1	0	32	0.984	0.016	agagacttgaaa[g/t]attatgaagctt	
A64588G		intron17	31	1	0	32	0.984	0.016	atgtgaggtaaa[a/g]aggaagttcttt	
T67183G		intron17	31	1	0	32	0.984	0.016	tttaattcctaa[t/g]aatacttgttt	rs5745767

Three SNPs underlined had the minor allele frequency over 10% and were selected for genotyping in this study.
* Six polymorphisms are in strong linkage disequilibrium (r-square > 0.5).